Physics – Uspekhi **68** (8) 823 – 842 (2025)

CONFERENCES AND SYMPOSIA

PACS numbers: 52.35.Vd, 52.40.Kh, **94.05. – a**

ON THE 100th ANNIVERSARY OF S.I. SYROVATSKII'S BIRTH

Current sheets in plasma: from theory to experiment *

A.G. Frank

DOI: https://doi.org/10.3367/UFNe.2024.09.039764

Contents

Abstract. The main stages of experimental studies of the dynamics and evolution of current sheets formed in plasma in strong nonuniform magnetic fields are reviewed. These studies were initiated by Sergei Ivanovich Syrovatskii, who made an outstanding contribution to the creation of the MHD theory of current sheets. The experiments were developed in close interaction with the theory and under the influence of theoretical ideas and concepts. It was found that, in high-conductivity plasma, the formation of a current sheet leads to a concentration of magnetic energy, while during explosive destruction of the sheet, the magnetic energy is converted into the energy of plasma and accelerated electrons. It is shown that in many cases the rupture of the sheet is triggered by a rapid local increase in the plasma temperature and a violation of the transverse equilibrium within the current sheet. It has been proven that current sheets can develop in 3D magnetic configurations, and the range of such configurations has been determined. Reverse currents are found to play an important role in limiting the duration of plasma flows accelerated in current sheets.

Keywords: current sheets, magnetic reconnection, solar flares, MHD theory, laboratory experiments, plasma dynamics, 3D magnetic configurations

A.G. Frank
Prokhorov General Physics Institute, Russian Academy of Sciences,
ul. Vavilova 38, 119991 Moscow, Russian Federation
E-mail: annfrank@fpl.gpi.ru

Received 30 June 2025
Uspekhi Fizicheskikh Nauk **195** (8) 875 – 895 (2025)
Translated by M.Zh. Shmatikov

1. Introduction

The study of the formation and evolution of current sheets in plasma was largely stimulated by the exploration of the physical nature of 'flare' phenomena in space plasma, which are characterized by the rapid conversion of magnetic field energy into thermal and kinetic energy of the plasma and into flows of high-energy charged particles. The best known and well-studied phenomena of this kind are flares in the solar corona, grandiose events with the release of energy up to $\approx 10^{33}$ erg, a duration of about $\approx 10^2 - 10^3$ s, and the generation of accelerated particles with energies exceeding 100 MeV.

As a result of numerous long-term observations of solar flares, it was established that they usually occur in active regions of the Sun with strong nonuniform magnetic fields and a complex magnetic structure, including in areas where the polarity of the magnetic field alters and the magnetic field becomes zero [1, 2]. The reservoir of colossal energy released during flares is the magnetic field energy associated with electric currents flowing in the solar corona.

The data from astrophysical observations initiated theoretical studies. Stationary models of plasma flows in the vicinity of zero magnetic field lines were proposed, in which the transformation of magnetic energy into thermal plasma energy was considered [3–5]. However, stationary models fail to provide a satisfactory interpretation of the entire set of phenomena observed during solar flares, especially the generation of high-energy charged particles.

S.I. Syrovatskii formulated a general two-dimensional problem of nonstationary flows of high-conductivity plasma arising from the initial equilibrium state in a nonuniform

* The review is based on a talk given at the Scientific Session of the Physical Sciences Division of the Russian Academy of Sciences on 5 March 2025 (see *Phys. Usp.* **68** (8) 745 (2025); *Usp. Fiz. Nauk* **195** (8) 793 (2025)).

magnetic field with a zero line [6, 7]. This problem was considered in the approximation of a strong magnetic field using the equations of magnetohydrodynamics. The nonstationary plasma dynamics, which lead to the accumulation of excess magnetic energy in the vicinity of the zero line, were discussed in close connection with the possibility of the emergence of conditions for the generation of strong electric fields and effective acceleration of charged particles.

2. Theoretical concepts of formation of current sheet in vicinity of zero line of magnetic field

The development of a current sheet in the vicinity of the zero line of a magnetic field was considered in detail in [6, 7]. At the initial moment of time, a plasma at rest with a constant density and pressure is in a 2D magnetic field with a zero line. The magnetic field lines lie in the plane (x, y), and the zero line is aligned with the z-axis. In the vicinity of the simplest first-order zero line (Fig. 1), the field strength **B** increases linearly with distance **r** from the zero line:

$$\mathbf{B} = \{B_x;\, B_y;\, B_z\} = \{-hy;\, -hx;\, 0\}\,, \quad |\mathbf{B}| = h\,|\mathbf{r}|\,; \qquad (1)$$

here, h is the magnetic field gradient in the plane (x, y). The plasma density ρ and pressure p are constant, and the velocities **v** and electric current density **j** are zero:

$$\mathbf{v} = 0\,, \quad \mathbf{j} = 0\,, \quad \rho = \text{const}\,, \quad p = \text{const}\,. \qquad (2)$$

As follows from the exact solution obtained in the linear approximation [6, 7], the perturbation of the initial state, which arose far from the zero line, then propagates through the plasma in the form of a magnetosonic wave with a local velocity close to the Alfvén velocity:

$$|\mathbf{v}_\mathrm{A}| = \frac{h\,|\mathbf{r}|}{(4\pi N_\mathrm{i} M_\mathrm{i})^{1/2}}\,. \qquad (3)$$

Here, N_i and M_i are the concentration and mass of the plasma ions. As the wave approaches the zero line, its propagation velocity (3) decreases, while the amplitudes of all perturbations carried by the wave: magnetic field, current density, plasma velocity, and density increase. Thus, at a certain stage, the wave becomes nonlinear.

The motions of matter in the wake of the wave front are two-dimensional, and in two opposite quadrants of the plane (x, y) the plasma flows are directed from the periphery to the zero line, while in the other two quadrants, from the zero line to the periphery (see Fig. 1). In the conditions of the magnetic field being frozen into the substance, the plasma motion from the regions of a strong magnetic field to those of a weak field should lead to the magnetic field strengthening near the zero line, i.e., they should have a cumulative nature. As a result, the magnetic field lines should concentrate near the zero line, which is the 'stagnation point.'

The divergent nature of plasma flows (see Fig. 1) leads to the field lines of opposite directions being stretched near the plane $(y = 0)$, and the strengthening of the magnetic field can be accompanied by a decrease in the plasma density. Favorable conditions for the generation of induction electric fields and acceleration of charged particles can arise [6].

The exact solution to this problem in the linear approximation is valid, strictly speaking, only at a significant distance from the zero line. However, this solution displays the main trends in the variation of all quantities during plasma flows in a magnetic field with a zero line.

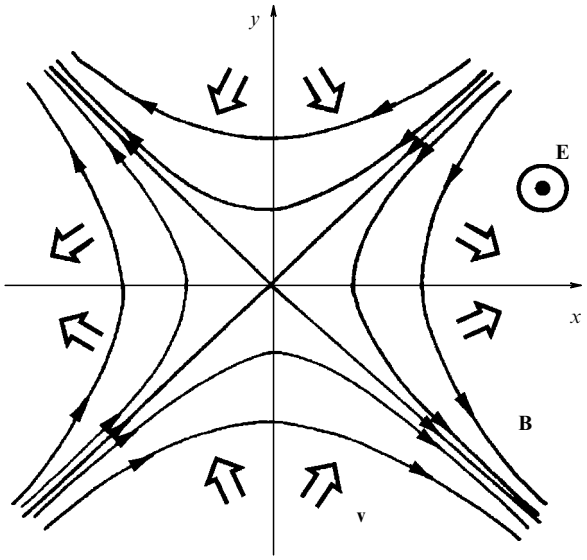

Figure 1. Two-dimensional magnetic field with zero X-line; plasma velocities are shown by double arrows.

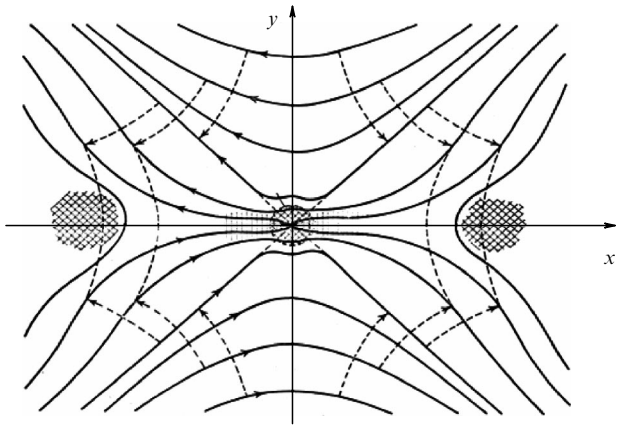

Figure 2. Pattern of magnetic field deformation in vicinity of zero line based on properties of freezing-in and continuity of magnetic field lines [6].

Based on the exact solution obtained in the linear approximation and a number of physical considerations, S.I. Syrovatskii proposed a qualitative picture of the magnetic field deformation that occurs during plasma flows with a frozen-in magnetic field in the vicinity of the zero line of the magnetic field (Fig. 2) [6]. Such a structure of the magnetic field actually corresponds to the concentration of magnetic energy in the vicinity of the zero line and the formation of a current sheet. In the case of rapid destruction of the sheet, it may be possible to transform the magnetic energy into the energy of plasma and accelerated particles.

The formation of a current sheet during plasma flows in the vicinity of the zero line of the magnetic field was substantiated in subsequent studies by S.I. Syrovatskii and his colleagues [8–12], in which it was shown that the current at the nonlinear stage takes the form of a thin sheet separating magnetic fields equal in magnitude and oppositely directed. Accurate nonlinear self-similar MHD solutions corresponding to a magnetic collapse process were obtained, with the

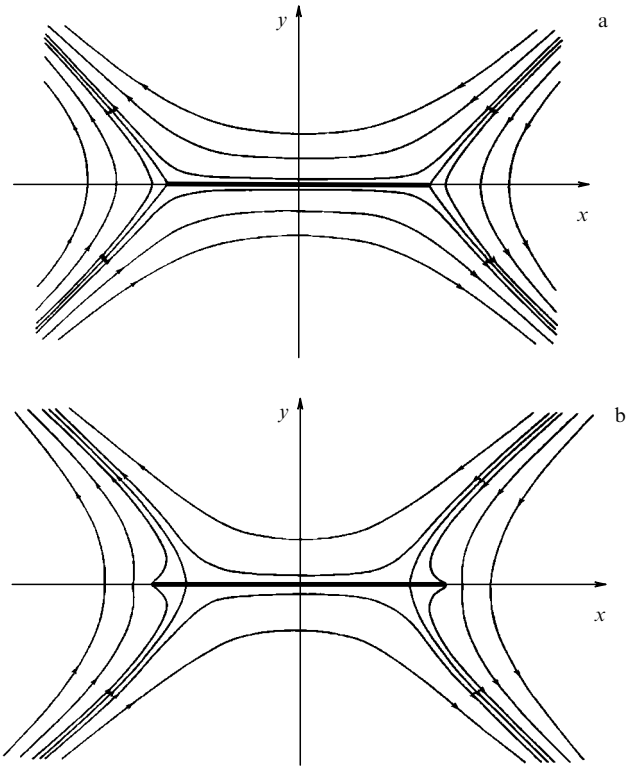

Figure 3. Current sheets developing in vicinity of zero line of magnetic field (shown as thick horizontal lines); thin curves are magnetic field lines. (a) Current sheet with current flowing in one direction; (b) current sheet with reverse currents at lateral ends of sheet [10].

magnetic field gradients and plasma density turning to infinity and a current sheet forming in a finite time [8, 9]. Rarefaction of the plasma near the surface of the current sheet was demonstrated in [11–13].

In [10], in the strong magnetic field approximation, it was established that, under conditions of a magnetic field frozen in the plasma, the appearance of an electric field directed along the zero line inevitably leads to the formation of a neutral current sheet. Note that the normal component in the neutral current sheet is absent, $B_y \approx 0$. Analytical expressions were derived for the structure of the magnetic field of the neutral current sheet, and it was shown that both direct and reverse currents can be present in the current sheet (Fig. 3). For a current sheet without reverse currents, simple relationships were obtained between the magnetic field gradient h, the total current in the sheet J and the half-width of the sheet b, and the dependence of the tangential component of the magnetic field B_x near the sheet surface on the distance $|x|$ to the zero line [10]:

$$hb^2 = \frac{4J}{c}\,, \tag{4}$$

$$B_x \approx hb\left(1 - \frac{x^2}{b^2}\right)^{1/2}. \tag{5}$$

These relationships were later used to estimate the parameters of the current sheets that were formed in the experiments.

It should be noted that the concept of the formation of a current sheet in the course of plasma flows in a magnetic field with a zero line was not generally recognized in the 1960s–1970s. The stationary Petschek model with four slow shock waves was very popular, especially among foreign physicists [5]. However, the following question was very urgent: what structure is formed in the vicinity of the zero lines — a current sheet or a Petschek flow? S.I. Syrovatskii proved that, under given boundary conditions, plasma flows arising in a magnetic field with a zero line are nonstationary and must inevitably lead to the formation of a current sheet [12].

One of the differences between a current sheet and Petschek flow is the structure of the magnetic field and electric current in the central region, i.e., in the vicinity of the zero line. In the current sheet, the current density in this region is maximum, in contrast to the local minimum in the Petschek model. This implies that this dilemma could be resolved if the structure of magnetic fields that are formed as a result of plasma flows in a magnetic field with a zero line is examined in detail. Such studies can be carried out, for example, using laboratory experiments.

3. Beginning of experimental studies. Neutral current sheet

Based on the ideas proposed by S.I. Syrovatskii [6, 7], experiments were started in the accelerator laboratory of the Lebedev Physical Institute to test the conclusions of the theory and clarify the options of converting the energy of a magnetic field into the energy of high-energy charged particles. It should be noted that, in the 1970s, experiments studying processes in the vicinity of zero lines of the magnetic field were started almost simultaneously in the USA [14], Japan [15], and in USSR, at the Lebedev Physical Institute [16].

The basic scheme of the experimental setup developed at the Lebedev Physical Institute (Fig. 4) included three different systems that operated independently, which made it possible to change the experimental conditions within fairly wide limits [17, 18]. Using straight conductors with currents which are located parallel to the axis of a cylindrical quartz vacuum chamber (6 cm in diameter and 60 cm in length), a quasi-stationary 2D magnetic field was created with lines of force in the plane (x, y), a zero line on the z-axis, and a gradient $h = (0.5-2)$ kG cm^{-1}:

$$\mathbf{B}^0 = \{B_x^0;\, B_y^0;\, B_z^0\} = h\{-y;\, -x;\, 0\}\,. \tag{1'}$$

In this field, the initial plasma was produced. Then, when pulsed voltage was applied to the gap between two electrodes introduced into the vacuum chamber from the ends at a distance of 40 cm from each other, an electric current was excited in the plasma parallel to the zero line with an amplitude of $J_z \leqslant 20$ kA, which ultimately should have led to the development of a current sheet.

The first experiments, conducted in a relatively rare plasma with an electron concentration of $N_e^0 \approx 10^{12}$–10^{13} cm^{-3}, revealed a fundamental problem on the way of formation a current sheet in laboratory conditions, in the vicinity of which a significant reserve of magnetic energy can accumulate. Excitation of an electric current led to the development of plasma instabilities and a sharp decrease in conductivity, which became abnormally low, $\sigma \approx (2-4) \times 10^{12}$ s^{-1}, i.e., significantly lower than the Coulomb conductivity, and featured a 'turbulent' character [16, 17]. As a result, at this stage, it was not possible to fulfill the condition of freezing the magnetic field into the plasma, which is

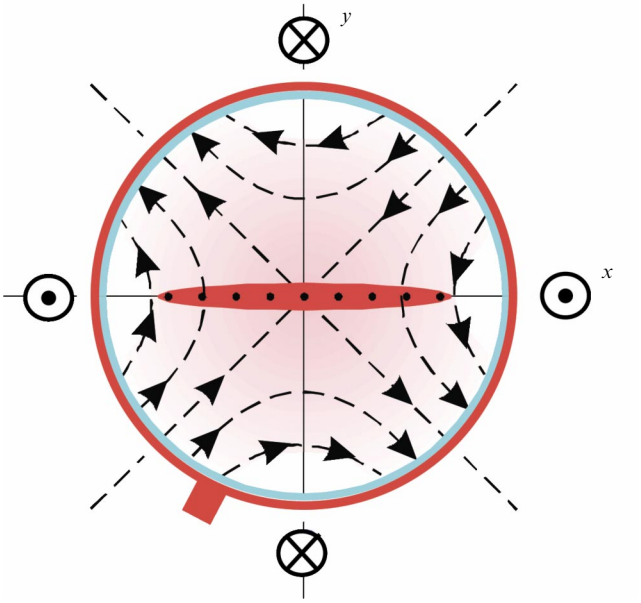

Figure 4. Current Sheet setup (FIAN) (cross section). A 2D magnetic field with field lines in (x, y) plane and zero line on z-axis was created by currents in four straight conductors located parallel to vacuum chamber axis. Current sheet was formed by exciting electric current J_z in plasma parallel to zero line.

necessary for concentrating magnetic energy during the formation of a current sheet.

The freezing of the magnetic field into a substance is usually characterized by a dimensionless parameter — the magnetic Reynolds number

$$\mathrm{Re_m} = \frac{4\pi\sigma l v}{c^2} \,. \qquad (6)$$

Here, v is the velocity of the substance, l is the characteristic size, and σ is the conductivity of the plasma. If $\mathrm{Re_m} \gg 1$, then, when matter moves from one region to another, the magnetic field is also transported. In the case of space objects, due to their gigantic scale, the freezing condition is satisfied for almost any conductivity, whereas in laboratory conditions the plasma conductivity value is critical.

It could be assumed that an increase in the density of the initial plasma would lead to an increase in conductivity [18]. Some experiments [19–21] showed that, with an increase in the electron concentration N_e, turbulent conductivity increases proportionally to $(N_e)^{1/2}$. On the other hand, an increase in the plasma density and, consequently, the frequency of Coulomb collisions could lead to the suppression of plasma instabilities.

To create a sufficiently dense initial plasma in a nonuniform magnetic field (1′), a special system was developed in the form of a high-voltage theta discharge with strong preliminary ionization [18]. The vacuum chamber was filled with a neutral gas, He or Ar, in which a breakdown was carried out, which made it possible to obtain plasma with a density of $N_e^0 \gg 3 \times 10^{14}$ cm^{-3} and to vary the mass composition of the plasma.

Indeed, an increase in the density of the initial plasma led to a significant increase in the average conductivity, which was $\sigma \approx 2 \times 10^{14}$ s^{-1}. As a result, it was possible to fulfill the condition of freezing the magnetic field into the plasma in a time interval of ≈ 1.5 μs, which exceeded the time of development of the current sheet.

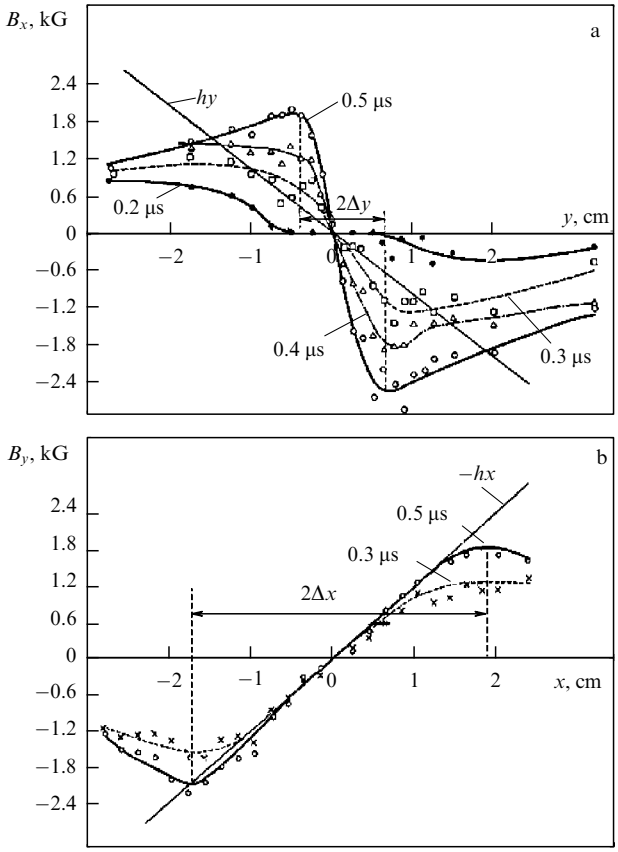

Figure 5. Spatial distributions of two components of magnetic field generated by excitation of current J_z in plasma at successive moments of time, (a) $B_x(y)$, (b) $B_y(x)$. Experimental conditions: $h = 1.2$ kG cm^{-1}, helium, $p = 10^{-2}$ Torr, $J_z^{\max} \approx 14$ kA.

An increase in the density of the initial plasma also led to an increase in the characteristic time of development of the current sheet, which made it possible to trace its formation. The process of formation of the current sheet and its characteristics were studied based on measurements of magnetic fields that were produced by an electric current flowing in the plasma (Fig. 5) [22].

Figure 5a shows the spatial distributions of the tangential component of the magnetic field $B_x(y)$ at successive moments in time. The moment $t = 0.2$ μs corresponds to the stage of magnetosonic wave propagation, when the magnetic field perturbations that arose at the lateral plasma boundaries at $t = 0$ have not yet reached the zero line ($y = 0$). At $t \approx 0.3$ μs, when the wave approached the zero line, the current sheet began to form. In the interval $t \approx 0.3-0.5$ μs, the B_x component of the magnetic field, and the derivative $\partial B_x/\partial y$, rapidly increased in the vicinity of the zero line, which indicated an increase in the plasma current density j_z, which at $t = 0.5$ μs reached a value of ~ 10 kA cm^{-2}. Concurrently, the size of region $2\Delta y$, where the plasma current is concentrated, decreased, i.e., this region was compressed to a value of $2\Delta y \approx 0.8$ cm. The B_x component of the magnetic field produced by the plasma currents exceeded the B_x component of the initial vacuum magnetic field, $B_x^0 = h\Delta y$, on the sheet surface by approximately fivefold (Fig. 5a).

Figure 5b shows the spatial distributions of the normal component of the magnetic field $B_y(x)$ at times $t \approx 0.3$ and 0.5 μs [22]. From a comparison of these curves, it is evident that the size of the region $2\Delta x$, in which the plasma current is

concentrated, increased with time, and at $t = 0.5$ μs it reached a size of $2\Delta x \approx 3.6$ cm.

Thus, in a finite time interval, the distribution of the plasma current in the plane (x, y) took the form of a sheet with a width-to-thickness ratio $\Delta x/\Delta y$ of 4.5, and, what is especially important, as a result of the formation of the current sheet, the magnetic energy density in the vicinity of the zero line significantly increased.

It should be especially emphasized that in experiment [22] a neutral current sheet was obtained with a normal component of the magnetic field, which was virtually zero. It follows from this observation that the magnetic field lines were extended along the surface of the current sheet, separating the oppositely directed magnetic fields (see [10] and Section 2). Indeed, as can be seen from Fig. 5b, within the width of the sheet, the normal B_y component of the magnetic field produced by the plasma current was equal in magnitude and directed oppositely to the normal component of the vacuum magnetic field, $B_y^0 = hx$. As a result, the actual, i.e., total, value of the normal component B_y^Σ was virtually zero:

$$B_y^\Sigma = B_y^0 + B_y = hx + B_y \approx 0\,. \tag{7}$$

The main parameters of the current sheet obtained in the experiment were in satisfactory agreement (with an accuracy of about 10%) with theoretical relations (4) and (5), which are characteristic of an infinitely thin neutral current sheet [10].

Based on magnetic measurements, it was also revealed that the current density is maximum in the central region of the sheet, i.e., in the vicinity of the zero line, and smoothly decreases towards the lateral edges of the sheet. This indicated that, in the vicinity of the zero line of the magnetic field, a current sheet was actually developing, rather than the Petschek flow. The formation of a neutral current sheet in the experiment was one of the important arguments for substantiating the concept of current sheets. Subsequently, the formation of current sheets was confirmed in other experiments [23], and was also substantiated in numerical calculations [24].

4. Stability of extended current sheets

According to the concept of S.I. Syrovatskii, the study of flare processes in plasma based on the dynamics of current sheets implies two main stages: first, obtaining a current sheet with a significant reserve of magnetic energy, and, second, implementing a rupture of the sheet with the conversion of the 'excess' magnetic energy into the energy of the plasma and accelerated particles [6, 7, 12]. The first stage was implemented experimentally, when a neutral current sheet was formed in a plasma of sufficiently high conductivity, and a significant increase in the magnetic field on the surface of the sheet, in comparison with the initial magnetic field, was obtained (Fig. 5a, b) [22].

It could be expected that, in the case of a rapid 'reconnection' of magnetic field lines through the sheet, i.e., during a macroscopic rupture of the current sheet, the excess magnetic energy would be transformed into the kinetic energy of the plasma and fluxes of accelerated particles. According to current concepts, the most probable cause of sheet rupture is tearing mode instability [25, 26]. As a result of the development of such instability, the current sheet disintegrates into separate current threads, and the magnetic field lines are reconnected through the sheet. The criterion for the development of the tearing mode is sufficient elongation of the current sheet:

$$\frac{\Delta x}{\Delta y} > 2\pi\,, \tag{8}$$

where $2\Delta x$ is the width of the sheet, $2\Delta y$ is its thickness, or the smaller transverse size of the sheet.

To obtain large current sheets and study the possibilities of breaking the current sheet and accelerating charged particles, the next generation Current Sheet setup, CS-3, was designed and produced [27, 28]. Similar to previous installations [17, 18, 29], the CS-3 setup included three independent systems: one for produced a 2D quasi-stationary magnetic field with a zero line, another for produced the initial plasma in this field, and the third for exciting electric current. The CS-3 setup was distinguished by its larger size, higher power characteristics, and an increased lifetime of the current sheet; it was also equipped with additional plasma diagnostic methods.

An increase in the size of the setup and, most importantly, an increase in the total current J_z flowing in the plasma, according to Eqns (4) and (5), should have provided a noticeable increase in both the width of the current sheet $2\Delta x$ and the magnetic energy reserve in the vicinity of the sheet. It was assumed that the thickness of the sheet $2\Delta y$ would not undergo significant changes compared to the previous series of experiments, and this would allow condition (8) to be met with a reserve. Indeed, as was found using magnetic measurements, the CS-3 setup enabled forming current sheets, the width of which was more than an order of magnitude greater than the thickness [27, 28], which ensured the fulfillment of condition (8).

It was found that the formation of a current sheet was accompanied by effective compression of the plasma into a flat extended plasma sheet, so that, as a result, the electron density N_e in the sheet was 5–10 times greater than the concentration of both the initial plasma and the plasma surrounding the current sheet [30, 31]. Figures 6a, b show a typical plasma interferogram obtained by holographic interferometry [32], and the corresponding 2D distribution of the electron density in the plane (x, y). Figures 6a, b clearly demonstrate that the plasma density distribution was virtually uniform along the width of the plasma sheet, while the width of the sheet significantly exceeded its thickness.

The structure of the plasma sheet, and in particular the sharp gradient concentration in the y direction transverse to the sheet, indicate that the gas-kinetic pressure of the plasma concentrated in the sheet was balanced by the magnetic pressure outside the sheet:

$$N_e^{\max}\left(T_e + \frac{T_i}{Z_i}\right) = \frac{(B_x^\Sigma)^2}{8\pi}\,. \tag{9}$$

Here, $N_e^{\max}$ is the maximum electron density, T_e and T_i are the electron and ion temperatures in the midplane of the current sheet, Z_i is the effective ion charge, and B_x^Σ is the tangential component of the magnetic field on the surface of the sheet. From Eqn (9), it follows that, under typical conditions, the effective plasma temperature in the sheet was $(T_e + T_i/Z_i) \approx (40-60)$ eV [27, 28].

Experiments using the CS-3 setup revealed that the extended current sheet existed in a stable state, without

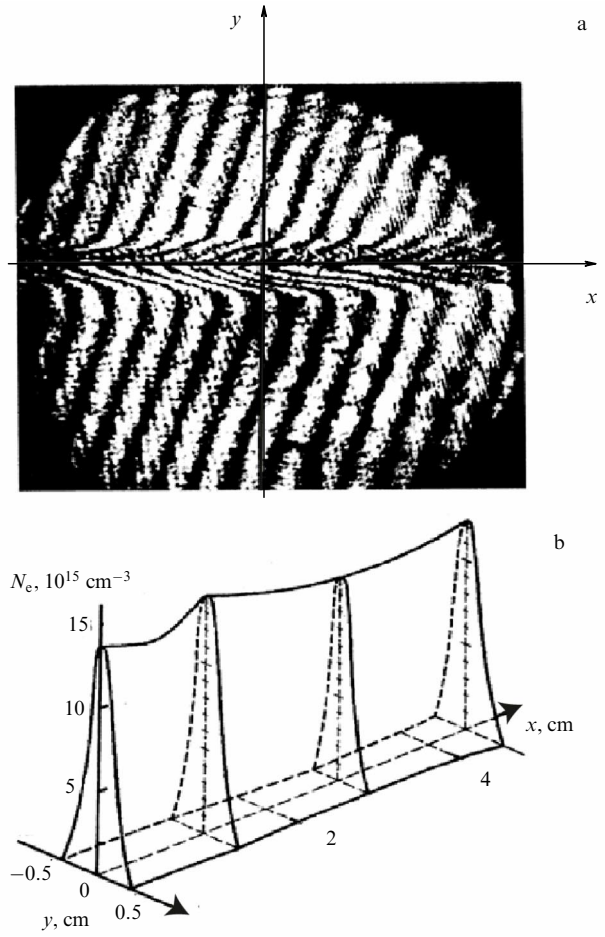

Figure 6. (a) Holographic interferogram of current sheet plasma recorded in CS-3 setup. (b) Two-dimensional distribution of electron density $N_e(x, y)$ obtained as a result of processing this interferogram. Experimental conditions: $h = 0.6$ kG cm^{-1}, helium, $p = 4 \times 10^{-2}$ Torr, $J_z^{max} \approx 40$ kA, $t \approx 1.1$ μs.

noticeable variation in its structure and parameters, for a long period of time, at least an order of magnitude greater than the characteristic time of tearing instability development [25, 26]. This implies that, in the experiments conducted, it was not possible to break the extended current sheet. However, as S.I. Syrovatskii emphasized, the high stability of current sheets is important for astrophysical applications, since it provides a mechanism for accumulating a significant amount of magnetic energy, which can then be released during a flare [33].

Thus, due to the stability of the extended current sheets formed in laboratory conditions, a problem arose with the implementation of the sheet break. It could be assumed that a significant role in stabilizing the discontinuity was played by the comparatively rarefied peripheral plasma surrounding the current sheet, and as soon as the discontinuity began, it was 'healed' due to the peripheral plasma flowing into the discontinuity [12, 34, 35]. A number of theoretical studies have shown that the discontinuity of the current sheet could be prevented by such factors as the finite conductivity of the peripheral plasma [36] and the plasma flows along the surface of the current sheet [37, 38].

The dynamics of the peripheral plasma in the vicinity of current sheets was studied experimentally by the phase location method using microwave radiation with wavelengths of 8 and 2 mm [29]. The velocities of both the inflow of peripheral plasma into the current sheet and the outflow of plasma from the sheet were measured, depending on the initial conditions under which the sheet was formed. It was found that the peripheral plasma velocities increased with an increase in the gradient of the initial magnetic field h, an increase in the amplitude of the current flowing in the sheet J_z, and a decrease in the density of the initial plasma. Based on the data obtained, such initial conditions were chosen that provided the highest velocities of the peripheral plasma flows in the vicinity of the current sheet. Indeed, under these conditions, after a relatively long stage of stable existence of the current sheet, the magnetic field structure spontaneously and rapidly rearranged, which then led to a macroscopic rupture of the sheet [27, 28, 39]. Thus, a fairly reproducible rupture of the current sheet was achieved, which made it possible to study its main features in subsequent experiments [40].

5. Pulsed phase of magnetic reconnection and electron acceleration

The rupture of the current sheet occurred quite dramatically and led to a cardinal change in all the parameters that were characteristic of the previous stable stage of evolution (Figs 7–9). Many of the manifestations of the current sheet rupture are similar to the processes occurring during the impulsive phase of solar flares and in other flare phenomena.

The impulsive phase of magnetic reconnection occurred, as a rule, in the central region of the current sheet, where the current density was maximum. The structure of the magnetic field altered qualitatively: the tangential component sharply decreased with a simultaneous increase in the component normal to the surface of the sheet [27, 28, 39–42]. Consequently, the magnetic flux crossing the middle plane of the sheet ($y = 0$) increased significantly, i.e., the rate of reconnection of oppositely directed magnetic field lines through the current sheet, which previously was the boundary between these fields (Fig. 7b), increased: $t \approx 1.2-1.3$ μs [42, 43]. At the same time, a local minimum of the electric current density arose in the central region of the sheet. Then, the region of enhanced magnetic reconnection and reduced current density propagated from the center of the sheet to both its lateral edges (Fig. 7c) with a velocity of $v_x > 10^7$ cm s^{-1}, almost an order of magnitude greater than the Alfvén velocity characteristic of a stable sheet [43]. As a result, the electric current previously concentrated in the sheet was ejected beyond its limits, i.e., rapid destruction of the current sheet was observed.

Concurrently with the pulsed phase of magnetic reconnection, destruction of the plasma sheet occurred, which can be seen from the rapid changes in the 2D distributions of the plasma density displayed in Fig. 8 [40, 44]. Distributions in the form of lines of equal plasma density $N_e(x, y) = \text{const}$ at successive moments of time were recorded in one pulse of operation of the CS-3 experimental setup using the cine-holographic interferometry method [45–47]. The first frame in Fig. 8 ($t = 1.40$ μs) corresponds to a stable stage of evolution, when the plasma density distribution along the width of the sheet was almost uniform. The second frame ($t = 1.46$ μs) shows the appearance of an explosive expansion in the middle of the plasma sheet. The next three frames ($t = 1.52$, 1.58, and 1.64 μs)

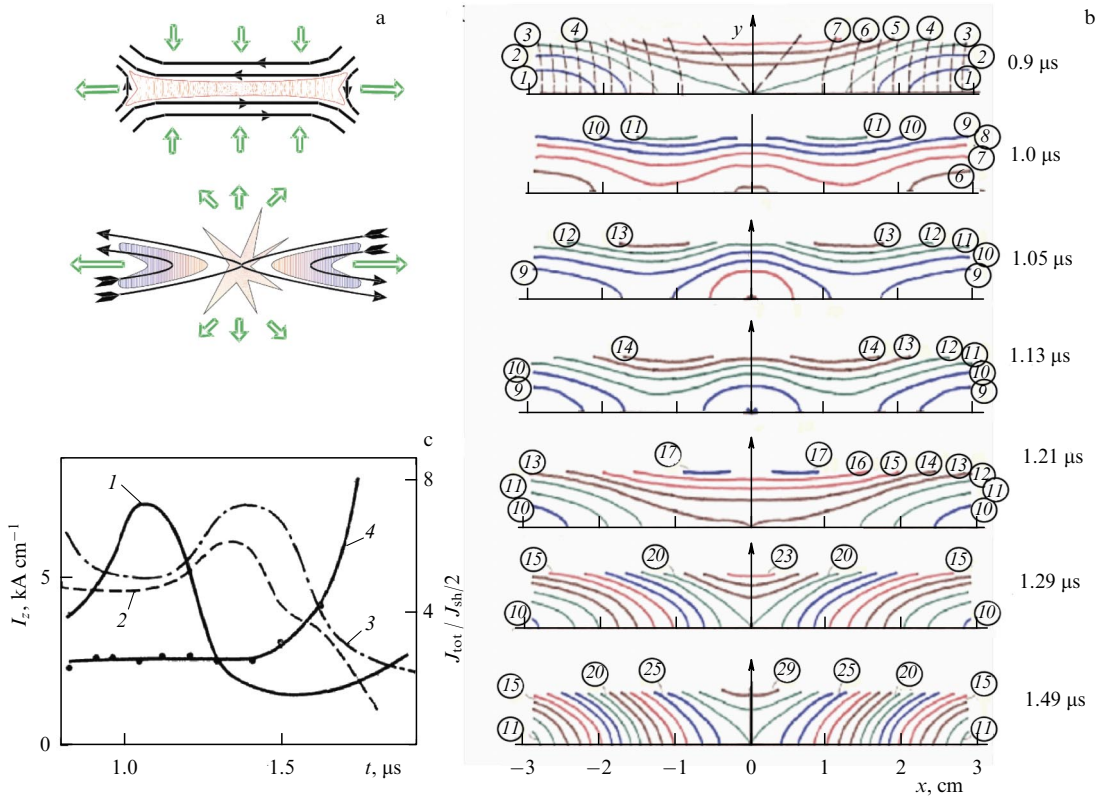

Figure 7. (a) Schematic of stable current sheet and explosive destruction of the sheet. (b) Structure of magnetic field lines of current sheet at successive moments of time (half of sheet cross section is shown). Numbering of field lines is continuous for all moments of time, interval between lines is 250 G cm. Dashed curves are field lines of 2D vacuum magnetic field (1). (c) Time dependence of linear current density in different sections along current sheet width: *1* — $x = 0-0.5$ cm; *2* — $x = 1-1.7$ cm; *3* — $x = 2.2-2.9$ cm; *4* — ratio of total plasma current to total current in half of current sheet. Experimental conditions: $h = 0.6$ kG cm^{-1}, helium, $p = 5 \times 10^{-2}$ Torr, $J_z^{max} \approx 40$ kA.

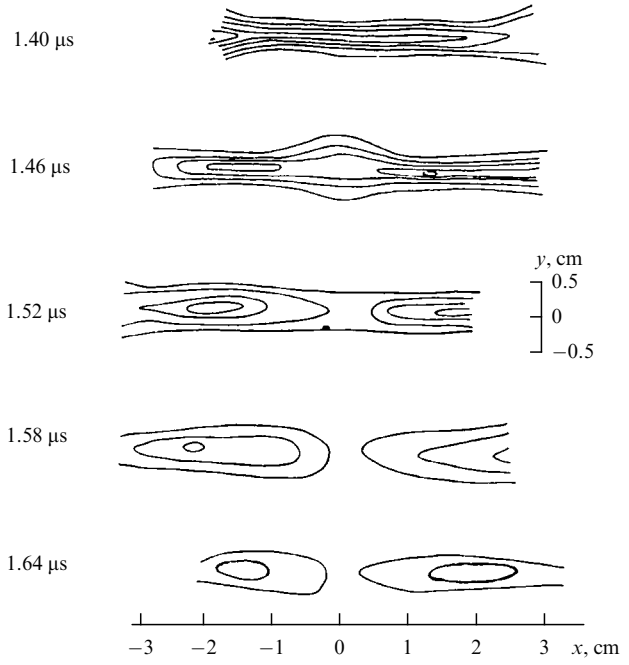

Figure 8. Spatial distributions of electron density $N_e(x, y)$ presented in the form of equidensity lines at successive moments of time at stage of explosive destruction of current sheet. Distributions were obtained by processing a 5-frame series of holographic interferograms recorded by cine-holography method. Adjacent contour lines correspond to change in electron density by $\Delta N_e = 1.25 \times 10^{15}$ cm^{-3}. Experimental conditions: $h = 2.0$ kG cm^{-1}, argon, $p \cong 10^{-2}$ Torr, $J_z^{max} \approx 30$ kA.

demonstrate a rapid decrease in both the plasma density and the total number of electrons in the sheet, suggesting that at this stage plasma flows were generated that ejected plasma beyond the sheet.

As a result of studying the dynamics of rapid changes in magnetic fields and electron density, a spatio-temporal correlation was found between changes in the structure of magnetic fields during the pulsed phase of magnetic reconnection, on the one hand, and the destruction of the plasma sheet, on the other hand [40, 44, 47]. It may be concluded that both of these processes represent different manifestations of the explosive destruction of the current sheet.

Rapid changes in magnetic fields during the pulsed phase of magnetic reconnection should inevitably lead to the excitation of induction electric fields. According to estimates, the induction field strength was $E^{ind} > 300$–400 V cm^{-1}, which usually exceeded the external initial electric field used to form the current sheet [39, 40, 43]. It was natural to assume that the excitation of induction electric fields in the current sheet during the pulsed phase of magnetic reconnection should be accompanied by the acceleration of charged particles. Indeed, accelerated electrons with energies reaching ≈ 10 keV were detected in experiment [48]. Using a multichannel X-ray sensor [49], the energy spectrum of accelerated electrons was also obtained. The analysis showed that the electron spectrum is non-Maxwellian and is significantly enriched in particles with energies exceeding 5–10 keV [48]. Within the measurement accuracy, the obtained spectrum of accelerated

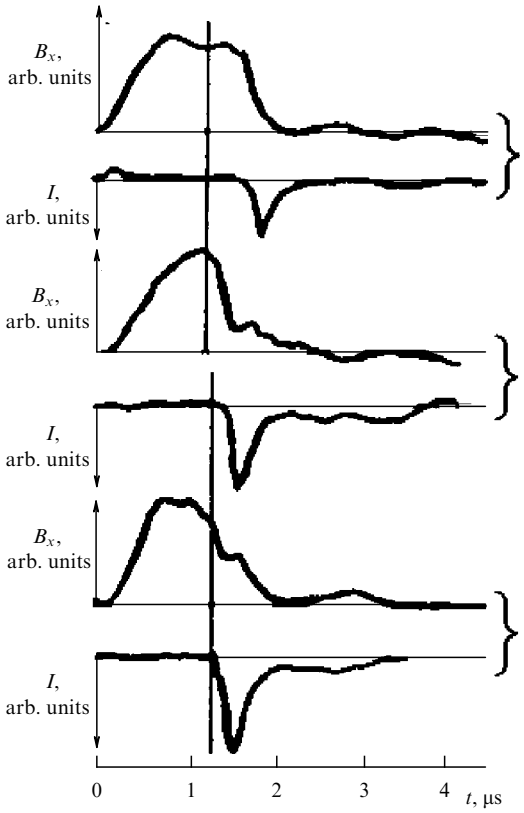

Figure 9. Time dependences of tangential B_x-component of magnetic field in central region of current sheet and signal of X-ray radiation detector I indicating generation of accelerated electrons. Three different pulses of CS-3 setup are shown. Experimental conditions: $h = 2.6$ kG cm^{-1}, argon, $p = 10^{-2}$ Torr, $J_z^{\max} \approx 30$ kA.

electrons could be satisfactorily approximated either by a steep power-law spectrum with the index $\gamma = -6-7$ or by an exponential spectrum close to the theoretically calculated spectrum of particles accelerated in the vicinity of the zero line of the magnetic field [50].

A clear correlation was revealed in time between the pulsed phase of magnetic reconnection and the appearance of accelerated electrons, which were recorded when and only when the magnetic field structure of the current sheet rapidly rearranged [48, 51]. In those modes when the sheet existed stably and during the time intervals before the onset of the pulsed phase of magnetic reconnection, no accelerated electrons were observed.

Simultaneous measurements of the tangential component of the magnetic field B_x and the signal of the X-ray detector, which corresponded to three different pulses of the CS-3 setup, are presented in Fig. 9. In different cases, the fast phase of magnetic reconnection began at different moments in time and X-ray bursts appeared synchronously [51]. Such a correlation implies that the destruction of the current sheet is a necessary condition for the generation of fast electrons, i.e., for the conversion of part of the magnetic energy into the energy of accelerated particles. The fastest electrons, with energies of ≈ 12 keV, arose at the very beginning of the pulsed phase of reconnection [51], which indicates a qualitative analogy between the acceleration of electrons during the rupture of the sheet formed under laboratory conditions and the features of particle acceleration during solar flares [33, 52].

6. Temperature of electrons and ions in current sheet and plasma turbulence

One of the most difficult issues was to identify the physical factors that cause the termination of the comparatively long metastable stage of the evolution of the current sheet and the transition to the pulsed phase of magnetic reconnection, i.e., to the rupture of the current sheet. S.I. Syrovatskii [33, 53] considered the instability of the tearing mode, a sharp local decrease in conductivity due to the development of plasma turbulence, and thermal instability caused by a violation of the thermal balance in the current sheet to be the mechanisms that could cause the destruction of the current sheet.

Experimental studies of the structure of the magnetic field within the current sheet allowed revealing that the pulsed phase of magnetic reconnection began to develop in the central region of the sheet, where the current density was maximum and where in many cases a structure of the magnetic island type, or O-type zero line, existed (see, for example, Fig. 7b, $t \approx 1.0-1.2$ μs [43]). These data indicated that the destruction of the current sheet was apparently not associated with the development of tearing mode-type instability [40].

Analysis of the structure of magnetic fields, electric currents, and electron density in current sheets showed that these parameters remained virtually unaltered throughout the metastable stage of sheet evolution, right up until the beginning of the pulsed reconnection phase. It should be especially emphasized that, in the central region of the sheet, the average current velocity of electrons remained constant at the level of $u_e \approx (2-3) \times 10^6$ cm s^{-1} both before the onset of sheet destruction and during its rupture [40, 44, 47]. The virtually constant value of the current velocity indicated that, in all likelihood, current instabilities could not cause an increase in the anomalous resistance of the plasma and, consequently, could not initiate the pulsed phase of magnetic reconnection.

However, a number of experimental facts indicated that, even during the stable stage of the evolution of the current sheet, the temperature of the plasma concentrated within the sheet gradually increased. The appearance of radiation in the spectral lines of doubly- and triply-charged impurity ions, the gradual increase in the intensities of such lines, and the 'burnout' of the spectral lines of the working gas–all these factors testified to an increase over time in both the electron temperature T_e and the effective charge of the ions Z_i [44, 47]. A gradual increase in the ion temperature T_i was also observed [54], and at each moment in time the ion temperature exceeded the electron temperature [47]:

$$T_i > T_e . \tag{10}$$

It is characteristic that the 'burnout' of the spectral lines of the working gas occurred predominantly in the middle plane of the sheet, and to the greatest extent in the center of the sheet [55, 56], i.e., in those areas where the current density was maximum.

During the formation and evolution of the current sheet, a sequential excitation of the spectral lines of ions of different ionization multiplicities was observed, and the higher the ion ionization degree, the later the radiation of the corresponding spectral line appeared [57]. Of particular interest were the short-term bursts of radiation in the spectral lines of multiply charged ions of carbon, nitrogen, and oxygen, which were

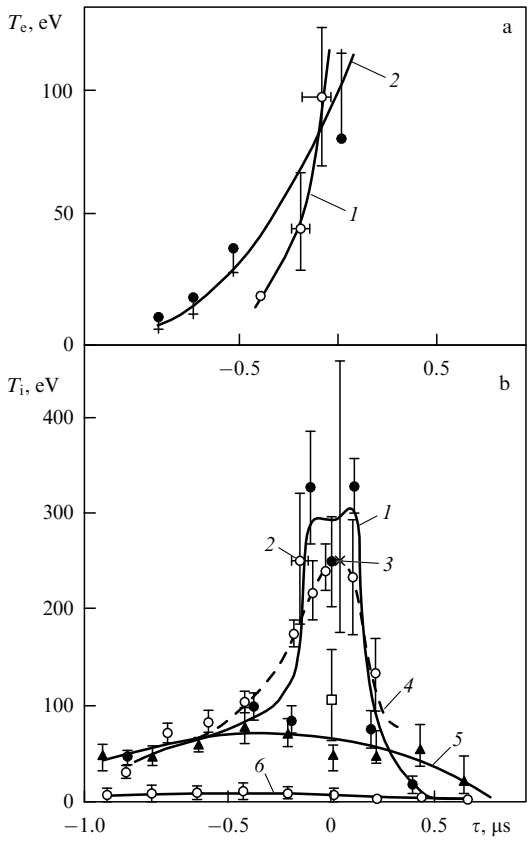

Figure 10. Time variations in electron temperature T_e (a) and ion temperature T_i (b) in central region of current sheet before onset of its destruction at $\tau \approx 0$. Curve *1* (panel a) obtained based on estimates of T_e from ionization time of oxygen ions OIV, OV, and OVI [57]; curve *2* based on time evolution of spectral lines of oxygen ions OII–OVI as a result of solving equations of ionization kinetics [59]. Ion temperature (panel b) was determined based on half-widths of profiles of various spectral lines: CIV 581.2 nm (*1*), NV 462.0 nm (*2*), OVI 381.1 nm (*3*), HeII 468.6 nm (*4*), CIII 464.7 nm (*5*), HeI 667.8 nm (*6*). Experimental conditions: $h = 0.6$ kG cm^{-1}, helium, $p \cong 5 \times 10^{-2}$ Torr, $J_z^{max} \approx 45$ kA.

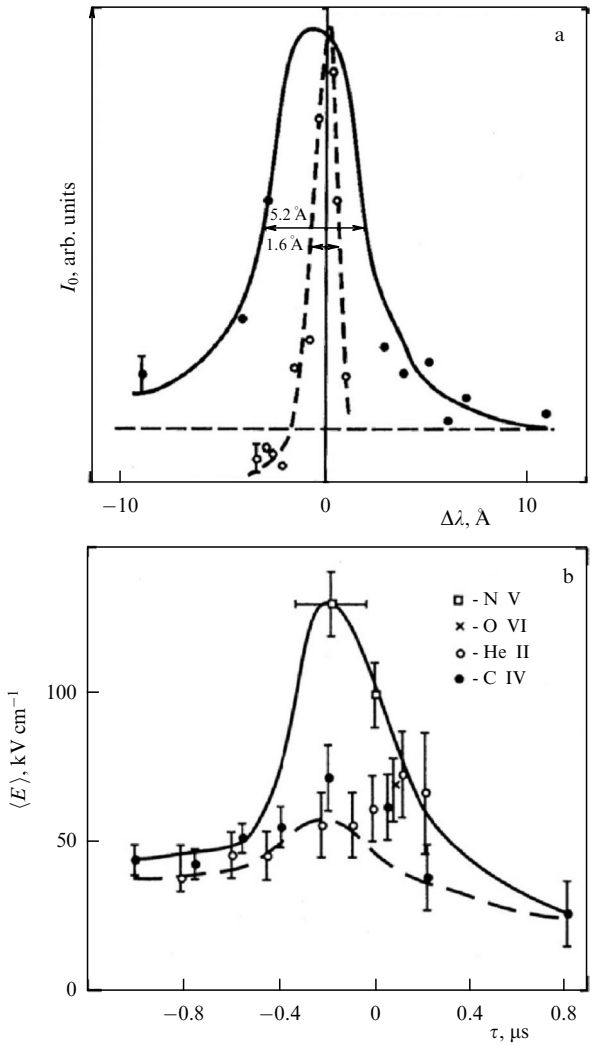

Figure 11. (a) Profiles of two spectral lines of nitrogen ion: NV 462.0 nm — dashed line; NV 494.5 nm — solid line, $t = 1.7$ μs. (b) RMS strength of anomalous electric fields in current-sheet plasma depending on time [61]. Experimental conditions: $h = 0.6$ kG cm^{-1}; helium, $p \cong 5 \times 10^{-2}$ Torr, $J_z^{max} \approx 45$ kA.

detected in the current-sheet plasma [57, 58]. The appearance of radiation in spectral lines with excitation potentials from 90 to 130 eV indicated a sharp increase in the electron temperature at a certain stage of the current sheet evolution. As a result of an analysis of the time dependences of the intensities of the spectral lines of oxygen ions, from OII to OVI, the electron temperature in the current sheet was calculated and its characteristic features were revealed [57, 59]. As can be seen from Fig. 10a, during the stable stage of sheet evolution, the electron temperature increased relatively slowly, in the range from ≈ 10 to ≈ 50 eV, and then T_e rapidly increased to a value of ≈ 100 eV [57, 59].

The maximum ion temperature reached even higher values immediately before the onset of the pulsed phase of magnetic reconnection (Fig. 10b) [58]. During the metastable stage, the ion temperature T_i gradually increased from 45 to 80 eV, and then a sharp rise in temperature to $T_i \approx 300$ eV occurred. The maximum values of ion and electron temperatures were reached almost simultaneously and immediately before the onset of current sheet destruction.

These results, along with the estimates made, allowed drawing a conclusion that intense plasma heating occurred in a relatively small region within the current sheet, or in a 'hot spot' [58, 60]. The appearance of a hot spot within the current sheet can naturally be compared with the formation of a magnetic island in the central region of the sheet, i.e., a configuration with closed field lines (see, for example, Fig. 7b $t \approx 1.05-1.13$ μs). It can be assumed that further plasma compression within the magnetic island led to a local increase in the thermal energy density, especially taking into account the probable decrease in plasma thermal conductivity [60].

The excitation of nonequilibrium electric fields in the dense heated plasma of the current sheet was detected by spectroscopy methods, when comparing the profiles of two different spectral lines of the same multicharged ion [57, 58, 61]. The lines were selected in such a way that the broadening of one of them was due predominantly to the Doppler effect, which made it possible to determine the ion temperature, while the other line was sensitive to both the Doppler effect and the Stark effect. As an example, Fig. 11a shows the profiles of two spectral lines of the four-charged nitrogen ion NV [57]. A comparison of the profiles of such pairs of lines, recorded experimentally, and the corresponding calculations made it possible to prove the appearance of anomalous

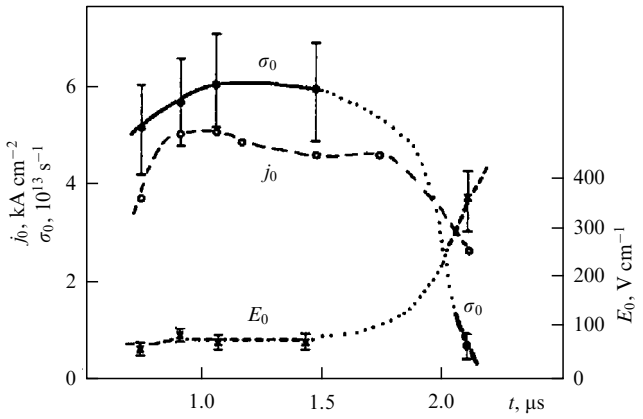

Figure 12. Time dependences of electric field E_0, current density j_0, and plasma conductivity σ_0 in vicinity of zero line of magnetic field.

electric fields in the current sheet plasma and to track the changes in their intensity at successive stages of sheet evolution (Fig. 11b) [61]. As a result, it was found that, during the metastable stage of the current sheet evolution, the root-mean-square strength of the anomalous electric fields was $\langle E\rangle \approx 50$ kV cm^{-1}, and the turbulence level, i.e., the ratio of the energy of the anomalous electric fields to the thermal energy of the plasma,

$$\eta = \frac{\langle E\rangle^2}{8\pi N_e \left(T_e + T_i/Z_i\right)}\,, \tag{11}$$

was $\eta \approx 10^{-3}$. By the end of the metastable stage, almost simultaneously with the sharp increase in the temperatures of electrons and ions, an increase in the electric field strength to $\langle E\rangle \approx 100$ kV cm^{-1} was observed. However, the level of turbulence did not increase and remained at the same level, i.e., $\eta \approx 10^{-3}$.

This implies that neither the constant level of turbulence nor the constant value of the current velocity of electrons could lead to a sharp decrease in the plasma conductivity before the rupture of the current sheet. These results show that the immediate cause that yielded the macroscopic destruction of the sheet was, in all likelihood, not associated with a local decrease in conductivity [40, 60, 62]. However, following the rupture of the current sheet, the plasma conductivity in the central region of the sheet decreased by approximately an order of magnitude (Fig. 12), i.e., in this case, the drop in conductivity appeared as a secondary effect [60].

Thermal processes associated with pulsed local heating of the plasma seem to be the most probable cause of the termination of the metastable stage of sheet evolution and the onset of the pulsed phase of magnetic reconnection. Based on experimental facts, the following sequence of phenomena can be assumed [58, 60]. In the central region of the sheet, a local maximum of the electric current and a system of closed magnetic field lines arose, i.e., a magnetic island, where first slow heating of the plasma occurred, followed by extremely rapid heating caused, in all likelihood, by compression of the substance. The growth of the gas-kinetic pressure of the plasma led to a violation of the transverse equilibrium of the current sheet (9), i.e., to a kind of thermal micro explosion, which was accompanied by expansion of the plasma at the speed of sound. This process initiated an increase in the reconnection rate of oppositely directed magnetic fields through the current sheet and a redistribution of the electric current in the sheet. As a result of the change in the magnetic field topology, the region of enhanced reconnection and reduced current density rapidly expanded along the surface of the sheet, from the center to the edges, which ultimately led to macroscopic destruction of the current sheet.

It should be noted that, in relation to current sheets in the solar atmosphere, S.I. Syrovatskii considered possible violation of the thermal balance after the temperature reaches a certain critical value, when the heating of the plasma can no longer be compensated for by radiation losses [63]. Despite the different nature of energy losses under laboratory experiment conditions and in the solar atmosphere, thermal processes very probably play a decisive role in the transition from the metastable stage of current sheet evolution to the rapid destruction stage.

7. Laboratory experiments and solar flares

Thus, S.I. Syrovatskii's concept of current sheets as the basis for flare phenomena in plasma has been experimentally confirmed. In laboratory conditions, it was possible to reproduce the main features of the flare process, namely the accumulation of magnetic energy over a relatively long period of time during the formation of a metastable current sheet followed by the rapid release of the accumulated energy during the rupture of the sheet. The rupture of the current sheet manifested itself in a sharp change in the topology of the magnetic field, the redistribution of the electric current, the destruction of the homogeneous plasma sheet, the generation of plasma flows, the excitation of induction electric fields, and the acceleration of charged particles. The analogy with solar flares was, in particular, reflected in the title of S.I. Syrovatskii's publication "Solar Flares in the Laboratory" [64].

Conditions in outer space and in laboratory experiments can naturally be compared in a quantitative way on the basis of characteristic dimensionless parameters that allow one to estimate the relative role of various physical factors in a particular phenomenon [65].

Due to the enormous difference in spatial scales in space and in laboratory setups, space phenomena can only be reproduced in laboratory conditions within the framework of limited modeling, when in both cases the corresponding dimensionless parameter is greater (or less) than unity [66–69]. The absolute values of the corresponding parameter can differ significantly up to several orders of magnitude.

A complete system of dimensionless parameters that characterize magnetohydrodynamic processes in 2D magnetic fields with zero lines was considered by S.I. Syrovatskii in [33, 35], where estimates and comparisons of dimensionless parameters for the solar corona and for a laboratory experiment were also presented.

For the analysis of magnetohydrodynamic flows of plasma with finite conductivity, without taking into account other dissipative processes, the following dimensionless parameters are usually used:

$$\beta = \frac{8\pi p}{B^2}\,,\ \varepsilon = \frac{v}{v_A} = \frac{\delta B}{B} \approx \frac{cE}{Bv_A}\,,\ \mathrm{Re_m} = \frac{lv_A}{\nu_m}\,,\ \tau = \frac{t}{t_A}\,. \tag{12}$$

Here, β is the ratio of the gas-kinetic pressure to the magnetic pressure; ε is the nonlinearity parameter, i.e., the relative

Table. Dimensionless parameters characterizing physical conditions in active regions of solar corona in laboratory experiment.

Parameters	Solar corona	CS-3
β	4×10^{-4}	$(0.4-6) \times 10^{-3}$
ε	$(0.4-2) \times 10^{-4}$	0.1
$\mathrm{Re_m}$	6×10^{13}	30 – 120
τ	6×10^{4}	15 – 3
L	$(0.24-2) \times 10^{10}$	3 – 12
S	0.2 – 1	$(0.33-5) \times 10^{2}$

magnitude of the magnetic field perturbation, or the ratio of the matter velocity to the Alfvén velocity v_A (3); $\mathrm{Re_m}$ is the magnetic Reynolds number (6), which characterizes the freezing of the magnetic field into the plasma; and τ is the ratio between the duration of the process t and the Alfvén time $t_A = (4\pi N_i M_i)^{1/2}/h$.

The special nature of plasma flows in nonuniform magnetic fields containing zero lines requires changing the dimensionless parameters (12), since they lose their meaning near the zero lines, where the values of B and v_A tend to zero. In a general analysis of the problem of plasma flows in the vicinity of zero lines of the magnetic field [35], S.I. Syrovatskii introduced two special dimensionless parameters L and S, which were subsequently called 'Syrovatskii numbers':

$$L = \varepsilon\,\mathrm{Re_m}\,,\ \ S = \frac{2\varepsilon}{\beta}\,. \tag{13}$$

The Syrovatskii numbers determine the nature of plasma flows in nonuniform magnetic fields containing zero lines and the possibility of forming current sheets that have a significant reserve of magnetic energy [70, 71]. The parameter L characterizes the relative increase in the magnetic field gradient as a result of the formation of a current sheet, while the parameter S determines the role of the directed velocities of plasma flows compared to the speed of sound.

The table displays the values of the dimensionless parameters characterizing the physical conditions in the active regions of the solar corona [52, 72] and in laboratory experiments [27, 28, 40]. As can be seen from the table, the dimensionless parameters characterizing typical conditions in the solar corona and in laboratory experiments satisfy the following strong inequalities:

$$\beta \ll 1\,,\ \varepsilon \ll 1\,,\ \mathrm{Re_m} \gg 1\,,\ \tau \gg 1\,,\ L \gg 1\,. \tag{14}$$

However, for the Sun, the number $S \leqslant 1$, while in laboratory conditions, S is usually > 1.

From this we can conclude that, within the framework of limited modeling, the experiments conducted at the Current Sheet installations have satisfactorily reproduced the physical conditions characteristic of the pre-flare situation on the Sun in terms of the possibilities of accumulating magnetic energy. In all likelihood, the experiments should also correctly reproduce the main features of flare processes.

8. Current sheets in 3D magnetic configurations

Two-dimensional inhomogeneous magnetic fields with zero lines (1) represent a certain idealization of more general 3D magnetic configurations. In real conditions, both in space objects and in installations for confining and heating plasma, magnetic fields usually contain all three components, i.e., are three-dimensional (3D). Therefore, the study of the possibilities of current sheet formation in 3D magnetic configurations and the analysis of the structural features of current sheets that can develop in such configurations are of fundamental importance.

Of considerable interest is the generalization of the results on the formation and evolution of current sheets that were obtained in 2D fields with zero lines to 3D magnetic configurations. Usually considered as 3D analogues of zero lines are singular or limiting field lines belonging simultaneously to several independent magnetic fluxes [3, 73] and closed field lines [74, 75]. As a result of perturbations of the initial equilibrium state of magnetized plasma, strong electric currents may appear in the vicinity of such lines [76].

The most apparent example of a magnetic configuration with a singular X-type line is the superposition of a 2D field with a zero line (1) and a longitudinal component B_z^0, which is directed along the zero line, changes relatively slowly in this direction, and is uniform in the plane (x, y):

$$\mathbf{B} = \{B_x;\, B_y;\, B_z\} = \{hy;\, hx;\, B_z^0\}\,, \tag{15}$$

$$\frac{\partial B_z^0}{\partial z} \ll h\,. \tag{16}$$

The formation of current sheets in magnetic configurations (15) and (16) was substantiated by S.I. Syrovatskii in studies [35, 76], in which he also showed that the presence of a longitudinal component leads to an effective increase in gas-kinetic pressure.

In a number of theoretical studies, based on self-similar solutions of the equations of magnetohydrodynamics, it was concluded that current sheets develop in 3D inhomogeneous magnetic fields in the vicinity of isolated zero points [77–80].

To study the possibilities of forming current sheets in various 3D magnetic configurations, the CS-3D setup (Fig. 13) was designed and created at the General Physics Institute of the Russian Academy of Sciences [81–83]. 3D magnetic configurations with topological features, such as zero points and singular lines, are created in the CS-3D setup by superimposing two magnetic fields with different types of symmetry, translational and axial [81]. The strengths of each field and the structure of the axial magnetic field can be changed independently of each other, which provides both a variety of 3D configurations (with one or more zero points, with singular lines, etc.) and a smooth transition from one configuration to another. In the selected 3D magnetic configuration, an initial plasma is produced, and then an electric current is excited, which initiates plasma flows and can lead to the formation of a current sheet.

When creating magnetic configurations (15) and (16), the transverse field gradient was $h \leqslant 1$ kG cm^{-1}, and the longitudinal component $B_z^0 \leqslant 8$ kG. A quartz vacuum chamber with a diameter of 18 cm and a length of 100 cm was filled with a noble gas (He, Ar, Kr), in which the initial plasma was produced. Then, an electric current with an amplitude of $J_z^0 \cong 40-50$ kA and a half-period of $T/2 \cong 6$ μs was excited in the plasma.

Experiments to study the possible development of current sheets in the vicinity of zero points confirmed the formation of current sheets in a wide range of 3D magnetic configurations with isolated zero points [82–86]. It was also found that

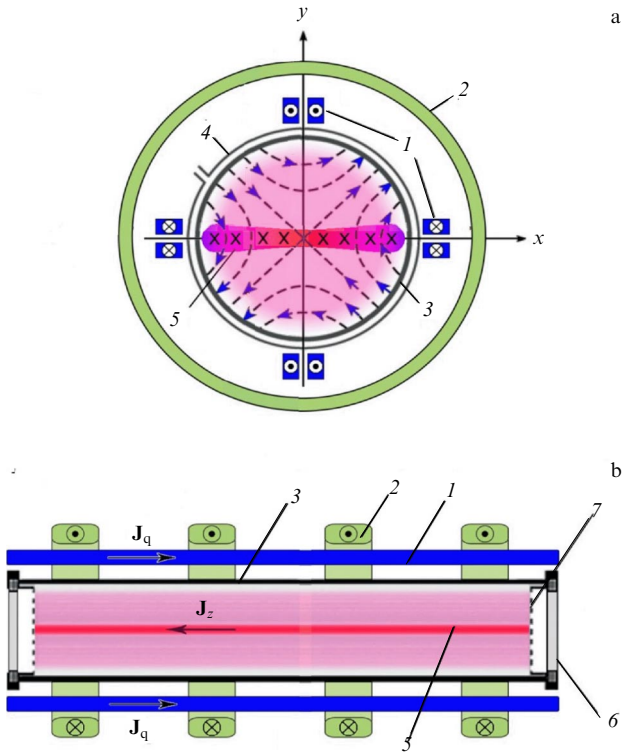

Figure 13. Schematic diagram of CS-3D experimental setup (GPI RAS): (a) cross section of the setup, (b) longitudinal section of the setup. *1* — straight conductors with currents for excitation of 2D (transverse) magnetic field with zero line $\mathbf{B} = h\{y; x, 0\}$; field lines of 2D field are shown in Fig. 1a by dashed lines with arrows; *2* — coils for excitation of axially symmetric magnetic fields; *3* — vacuum chamber $\varnothing = 18$ cm, $l = 100$ cm; *4* — theta discharge turns; *5* — current sheet; *6* — quartz windows; *7* — mesh electrodes.

current sheets are formed far from zero points, in areas with strong magnetic fields, and in 3D inhomogeneous magnetic fields without zero points [83, 85, 86]. In all cases, the necessary condition for the formation of the current sheet was the presence of a singular X-type line (15) in the 3D magnetic configuration.

Generally speaking, a 3D magnetic configuration with a singular X-line is a more general case compared to both 2D magnetic fields with zero lines and 3D fields containing zero points. In 3D configurations with isolated zero points, a singular X-line can be present both in the region of the zero magnetic field and far from this region. Therefore, a 3D configuration with a virtually uniform longitudinal component B_z^0 (15), (16) can be considered one of the elements of a more complex 3D magnetic configuration, the components of which vary in space.

In the 3D configuration (15), the magnetic field **B** never vanishes, while on the X-line both transverse components of the magnetic field, B_x and B_y, are equal to zero, as in the 2D configuration (1). This implies that, when studying the possible formation of a current sheet in 3D configurations with X-lines (15), (16), it is necessary first and foremost to determine the effect the longitudinal component B_z^0 can exert on the possible development of the current sheet and the changes with current sheets that may occur if they are formed in a 3D magnetic field in the presence of a longitudinal component.

Based on a number of experiments conducted using the CS-3D setup, it was concluded that current sheets can develop in 3D configurations with a sufficiently strong longitudinal component of the magnetic field directed along the X-line [85–90], as predicted in [35, 76]. The transverse dimensions of the current sheets being formed, width $2\Delta x$ and thickness $2\Delta y$, can differ from each other by a factor of 5 to 10, and, in this respect, current sheets in 3D magnetic configurations are very close to current sheets that develop in 2D fields with a zero line [91, 92].

The range of 3D magnetic configurations in which current sheets can be formed, in particular, the maximum value of the longitudinal component B_z^0 for a given value of the transverse gradient h, was determined. It was found that the ratio B_z^0/h should not exceed a certain critical value, which, in the experiments conducted at the CS-3D facility, was ≈ 15 cm [86, 89, 92]. Thus, current sheets can be formed in a fairly wide but limited range of 3D magnetic configurations with an X-line, and the most significant parameter determining the possibility of forming a current sheet is the gradient of the transverse magnetic field h [86, 92].

When comparing the current sheets that were formed in 3D magnetic configurations with an X-line (15), (16), significant differences were found in the current and plasma distributions across the sheet with a change in the strength of the longitudinal component B_z^0. With increasing B_z^0, a decrease in the maximum current density in the middle plane of the sheet and an increase in the sheet thickness $2\Delta y$ were observed (Fig. 14) [93]. Similar changes occurred with the plasma density distributions: with increasing B_z^0, the maximum electron density decreased and the plasma sheet thickness increased, while the total number of electrons per cm of the sheet width remained virtually unaltered [88, 90, 94]. These results showed that an increase in the longitudinal component B_z^0 in the initial 3D magnetic configuration with the X-line (15), (16) leads to a decrease in the degree of compression of the electric current and plasma within the sheet. This effect indicated a possible increase in the longitudinal component of the magnetic field in the sheet [87, 90].

Indeed, based on direct magnetic measurements, an increase in the longitudinal component of the magnetic field within the sheet was found, as compared to that outside the sheet (Fig. 15) [95]. The excess of the longitudinal component in the current sheet over the initial level B_z^0 was, depending on the conditions, $\delta B_z \cong (0.9-1.2)$ kG, and the direction of δB_z in all cases coincided with that of B_z^0 of the initial magnetic configuration.

As was reported in [95], at the stage of formation of the current sheet, perturbations of the longitudinal component of the magnetic field that arose at the periphery are transferred by plasma flows to the vicinity of the X-line, and, as they approach it, the amplitude of the perturbations increases. As a result, within the formed sheet, the longitudinal component is amplified compared to the initial level B_z^0. This effect indicates, in particular, that the magnetic field is frozen into the plasma. Note also that the longitudinal component is amplified within the entire width of the current sheet, both in the vicinity of the X-line and at a significant distance from it [95].

Unlike Eqn (9), the condition of transverse plasma equilibrium in the current sheet, taking into account the additional longitudinal magnetic field δB_z, should be presented as follows:

$$8\pi N_e^{\max}\left(T_e + \frac{T_i}{Z_i}\right) + (\delta B_z)^2 = (B_x^{\Sigma})^2 . \qquad (17)$$

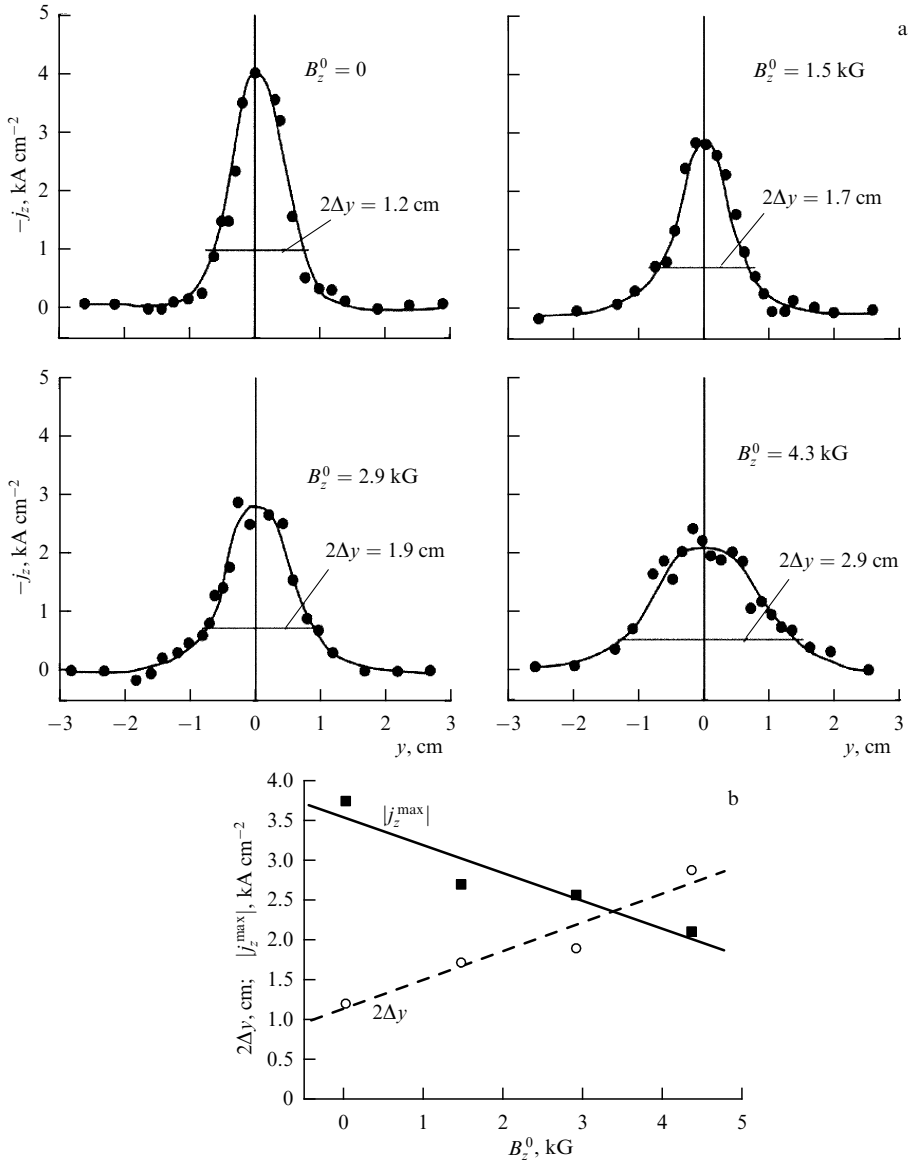

Figure 14. (a) Current density distributions $j_z(y)$ over current sheet thickness at various longitudinal field strengths $B_z^0 = 0$; 1.5 kG; 2.9 kG; 4.3 kG; (b) dependences of maximum current density j_z^{max} and current sheet thickness $2\Delta y$ at $0.25 j_z^{max}$ level on longitudinal field strength B_z^0. Experimental conditions: $h = 0.5$ kG cm^{-1}, argon, $p = 28$ mTorr, $J_z^{max} \approx 50$ kA.

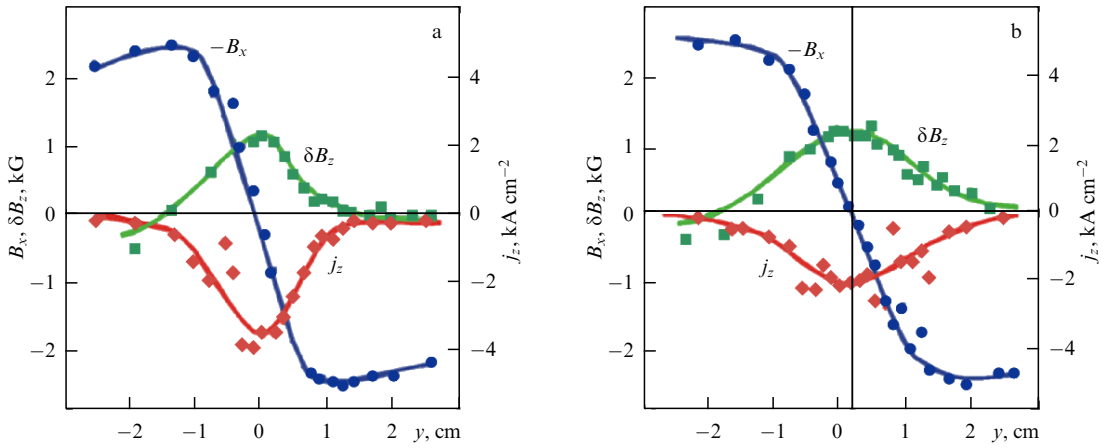

Figure 15. Distributions over current sheet thickness: tangential component of magnetic field B_x, current density j_z, and perturbation of longitudinal component δB_z for two values of initial longitudinal field: $B_z^0 = 1.5$ kG (a) and 4.3 kG (b). Experimental conditions: $h = 0.5$ kG cm^{-1}, argon, $p = 28$ mTorr, $J_z^{max} \approx 50$ kA.

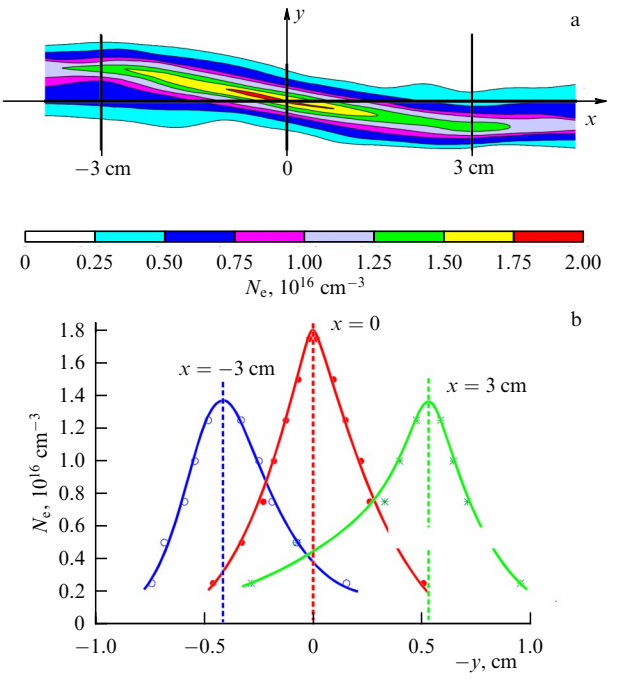

Figure 16. (a) Spatial distribution of electron density $N_e(x, y)$ in the form of lines of equal concentration in current sheet formed in 3D magnetic field (15), in the presence of uniform longitudinal component $B_z^0 \approx 3.0$ kG. (b) Distributions of electron concentration over plasma sheet thickness $N_e(y)$ for three different positions along sheet width: $x = 3$ cm; 0; −3 cm.

The pressure of the total magnetic field outside the sheet, $(B_x^{\Sigma})^2/8\pi$, should balance the sum of the gas-kinetic pressure of the plasma, $N_e^{\max}(T_e + T_i/Z_i)$, and the additional magnetic pressure $(\delta B_z)^2/8\pi$. This observation shows that the amplification of the longitudinal component of the magnetic field in the current sheet should lead (all other things being equal) to a decrease in the maximum electron density $N_e^{\max}$.

It is apparent that the amplification of the longitudinal component of the magnetic field in the current sheet formed in a 3D configuration with an X-line is provided by electric currents flowing in the transverse plane relative to the main current in the sheet. This leads to a significant complication of the current structure in the sheet, which becomes three-dimensional and differs significantly from the flat 'ribbon' current characteristic of current sheets formed in 2D magnetic fields with a zero line [96].

The influence of the longitudinal component of the magnetic field B_z^0 was also manifested in changes in the configuration of the current sheets, which in some cases became curved and asymmetrical (Fig. 16) [97–100]. The peripheral (lateral) regions of the current sheets deviated from the middle plane of the sheet in opposite directions, and these deviations were maximum at the early stage of the sheet evolution. Such asymmetry was found to arise as a result of excitation of Hall currents in the sheet and the appearance of additional dynamic effects during the interaction of Hall currents with the longitudinal component of the magnetic field B_z^0 [100–104].

Thus, experimental studies confirmed that current sheets can develop in various 3D magnetic configurations; however, both the spatial shape of the sheet and the structure of electric currents are significantly more complex than in the case of 2D magnetic fields with a zero line [92].

9. Plasma dynamics in current sheets

One of the most important properties of current sheets is that they are dynamic objects with intense plasma flows. Already the first stationary models [3–5] contained plasma flows that propagated through the current sheet, and the flow into the sheet was equal to the outgoing flow and was completely compensated by this flow. Nonstationary flows of compressible plasma during the formation of current sheets in the vicinity of singular magnetic field lines feature a much more complex nature (see, for example, [6–13, 35, 76]).

In experiments conducted at the Current Sheet installations, plasma flows were observed that arose at different moments in time and under different conditions, and in many cases the kinetic energy of the flows exceeded the thermal energy of the plasma concentrated in the current sheet [29, 40, 54, 60, 105–108]. Of considerable interest is the study of the physical factors under the effect of which plasma accelerates in current sheets and which affect the further evolution and parameters of plasma flows. To this end, the electrodynamic forces that arose in current sheets at various stages of their evolution were analyzed in [109–114]. The structure of electrodynamic forces was determined based on the spatial distributions of currents and magnetic fields in current sheets formed primarily in 2D magnetic configurations (1) with a zero line.

As noted above, the formation of a current sheet leads to a change in the initial magnetic configuration: the tangential component of the magnetic field B_x significantly increases and the normal component B_y decreases compared to the values of these components in the initial vacuum magnetic field. It is noteworthy that the real magnetic field **B** in the vicinity of the current sheet is the sum of the quasi-stationary field (1) and the magnetic field produced by the plasma currents. Figure 17 presents the distributions along the width of the current sheet of the tangential and normal components of the total magnetic field, $B_x(x)$ and $B_y(x)$, components B_x^0 and B_y^0 of the initial field (1), and the linear current density in the sheet $I_z(x)$ (see below). The normal component $B_y(x)$ is nonzero and has the same direction as the normal component of the initial magnetic field B_y^0.

As is known, plasma can be accelerated under the action of a gradient of gas-kinetic pressure and electrodynamic forces (Ampere forces):

$$M_i N_i \frac{d\mathbf{v}}{dt} = -\nabla p + \frac{1}{c}[\mathbf{j} \times \mathbf{B}]. \qquad (18)$$

Here, p is the gas-kinetic pressure of plasma, and $(1/c)[\mathbf{j} \times \mathbf{B}]$ is the density of Ampere forces. The Ampere forces acting in the y direction compress the current and plasma and lead to the formation of a current sheet, while the plasma pressure prevents compression. As a result, after the stage of current sheet formation, an equilibrium is established between the Ampere forces and the pressure gradient of the comparatively dense heated plasma concentrated in the sheet (see also Eqn (9)).

In the x direction, i.e., along the surface of the current sheet, the pressure gradient is usually negligible, and the plasma dynamics is determined primarily by the Ampere forces. In a 2D magnetic field of the current sheet, the density of the Ampere forces along the surface of the sheet depends on the magnitudes and directions of both the current density j_z and the normal component of the magnetic field B_y:

$$f_x(x, y, t) = -\frac{1}{c} j_z(x, y, t) B_y(x, y, t). \qquad (19)$$

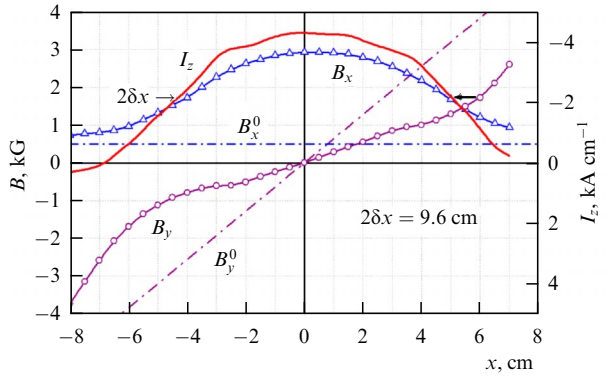

Figure 17. Distributions of tangential $B_x(x)$ and normal $B_y(x)$ components of current-sheet magnetic field and linear current density in sheet $I_z(x)$ along current-sheet width. Corresponding components of vacuum magnetic field: $B_x^0(x) = \text{const}$, $B_y^0(x) = hx$. Experimental conditions: $h = 0.57$ kG cm^{-1}, argon, $p = 28$ mTorr, $J_z^{\max} \approx 70$ kA, $t \approx 1.9$ μs.

This implies that the Ampere force acts on the plasma concentrated within the current sheet thickness $2\Delta y$ in the x direction:

$$F_x(x,t) = \int f_x(x,y,t)\,\mathrm{d}y = -\frac{1}{c}\,I_z(x,t)\,B_y(x,t)\,. \qquad (20)$$

Here, $I_z(x,t) = \int j_z(x,y,t)\,\mathrm{d}y$ is the linear current density in the sheet at $|y| \leqslant \Delta y$. It should be noted that within the integration region $2\Delta y$ the normal component B_y changes insignificantly (for more details, see [110]).

The distributions of the Ampere forces $F_x(x)$ along the surface of the formed current sheet and those of the linear current density $I_z(x)$ and the normal component $B_y(x)$ are displayed in Fig. 18a. The Ampere forces F_x are directed in opposite directions in two parts of the current sheet, at $x > 0$ and $x < 0$, namely, from the middle of the sheet to its two lateral edges. The absolute values of the Ampere forces increase with distance along the x-axis from the middle of the sheet to the periphery over most of the width of the sheet [110].

It is natural to expect that, in accordance with the structure of the forces F_x, the plasma be accelerated in the form of two differently directed flows that move along the width of the current sheet, from the middle of the sheet to its lateral edges, and the flow velocities increase with increasing distance from the middle of the sheet.

Accelerated plasma flows that arose in current sheets were detected and studied by spectroscopy methods [105–108, 111, 113]. Figure 18b presents a typical time dependence of the energy of directed plasma flows $W_x(t)$, from which it is apparent that there was a fairly large delay (≈ 2 μs) between the onset of current sheet formation and the appearance of directed plasma motions along the sheet surface. In the interval $t \approx 2-4.3$ μs, the plasma flow energy rapidly increased, and this energy significantly exceeded the thermal energy of the plasma. By the moment $t \approx 4$ μs, the average energy of the directed plasma motion reached $W_x \approx 400$ eV, while the ion temperature in the central region of the sheet did not exceed $T_i \leqslant 100$ eV. Then, after reaching a maximum, the energy of the flows rapidly decreased, i.e., the plasma flows that were accelerated in current sheets existed for a limited time.

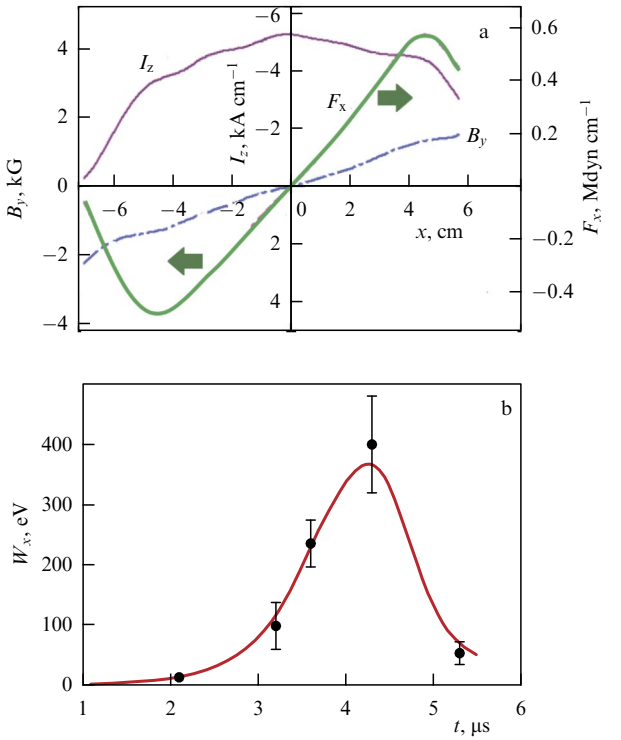

Figure 18. (a) Distributions of linear current density $I_z(x)$, normal component of current-sheet magnetic field $B_y(x)$, and Ampere forces $F_x(x)$ along current-sheet width. Arrows show directions of Ampere forces. Experimental conditions: $h = 0.63$ kG cm^{-1}, argon, $p = 28$ mTorr, $J_z^{\max} \approx 45$ kA, $t \approx 1.7$ μs. (b) Time dependence of energy of motion of accelerated plasma flows along current-sheet surface $W_x(t)$.

10. Excitation of reverse currents and their role in plasma dynamics

When studying the structure of the magnetic field in the vicinity of a current sheet formed in a 2D magnetic field with a zero line, S.I. Syrovatskii showed that, in the general case, the sheet can contain not only currents flowing in the direction of the external electric field E_z but also reverse currents arising at the lateral ends of the sheet (Fig. 3b) [10]. In the limiting case, the reverse currents could completely compensate for the main current, so the total current in the sheet would be zero; however, should this be the case, the reverse current density would significantly exceed the forward current density in the central region of the sheet. In [10], a situation was considered where the component of the magnetic field normal to the surface of the sheet was absent ($B_y = 0$); the magnetic lines of force of opposite directions did not intersect the infinitely thin current sheet, but were aligned along its surface, i.e., the sheet was 'neutral.'

To the best of our knowledge, the CS-3D setup was the first to experimentally detect reverse currents [110, 111]. When studying the distributions of the linear current $I_z(x,t)$ along the current sheet width, it was found that, at the late stages of evolution, currents in the opposite direction to the main current in the central part of the sheet arose at the lateral ends of the sheet (Fig. 19) [110]. The reverse currents were relatively small, and, over the time, their magnitudes increased somewhat, and the areas along the x-axis in which they are concentrated gradually expanded in the direction from the lateral edges to the middle of the sheet. It was found

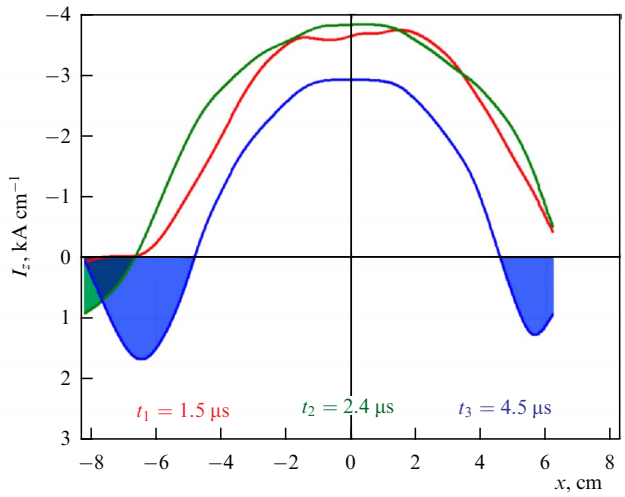

Figure 19. Distributions of linear current density $I_z(x)$ along current-sheet width at successive moments of time: $t_1 = 1.5$ μs; $t_2 = 2.4$ μs; $t_3 = 4.5$ μs. Experimental conditions: see caption to Fig. 17a.

that reverse currents can arise in a wide range of conditions, including during the development of current sheets in plasma with ions of different masses, but the moment of appearance of reverse currents and their magnitudes differed [115, 116].

At the late stages of evolution, along with the appearance of currents in the opposite direction, the transverse structure of the current sheet significantly altered, primarily in the peripheral regions. This was manifested both in a 'thickening' of the sheet, i.e., in an increase in its smaller transverse size, and in a more rapid decrease in the maximum current density at the periphery compared to the central region. Such changes almost coincided in time with the appearance of currents of the opposite direction at the lateral ends of the sheet [110, 111, 115, 116].

It is natural to assume that the appearance of reverse currents is associated with dynamic processes in current sheets, namely, with the propagation of fast plasma flows in the sheet. Indeed, the motion of plasma flows along the surface of the current sheet with velocities v_x in a transverse magnetic field B_y should lead to the excitation of induction electric fields $E'_z(x)$:

$$E'_z(x) = \frac{1}{c}\left(v_x(x)\, B_y(x)\right). \qquad (21)$$

The direction of the induction fields E'_z is opposite to the original electric field E^0_z, which excited the current J_z and led to the formation of the current sheet. It follows from Eqn (21) that the local value $E'_z(x)$ depends both on the plasma velocity $v_x(x)$ and on the strength of the normal component $B_y(x)$. In the central region of the sheet, the plasma velocities are small, but as the plasma moves from the middle of the sheet to the lateral edges, the velocities increase. The normal component B_y is also small in the center and increases significantly at the lateral edges of the sheet, at ($x \gg 0$). It follows that the electric fields $E'_z(x)$ arising from the motion of plasma flows must be substantially nonuniform within the current sheet and, most importantly, must increase sharply at the lateral edges of the sheet.

Thus, the motion of accelerated plasma flows with superthermal velocities v_x in the transverse magnetic field of the current sheet B_y must lead to the generation of induction electric fields E'_z, the magnitude of which is maximum at the lateral ends of the sheet and can exceed the initial electric field that caused the formation of the current sheet.

Under the action of induction fields $E'_z(x)$, electric currents j'_z of the direction opposite to the main current in the sheet j_z are excited in the current sheet. The superposition of the main and reverse currents leads to a decrease in the main current within the entire sheet; however, due to the nonuniformity of v_x and B_y, the manifestations of this effect are different in different regions. In the central region of the sheet, the electric fields E'_z and, consequently, the reverse currents j'_z are small; the main current is maximum, and the role of the reverse currents is insignificant. On the contrary, near the lateral edges, where the field strength E'_z increases significantly, the reverse currents j'_z should make a predominant contribution to the total current, given especially the decrease in the main current at the periphery of the sheet. Indeed, as follows from the experimental results, the reverse current appears, first and foremost, at the very edge of the current sheet.

The moment of the appearance of the reverse currents was determined by the time interval required for the acceleration of the plasma and the arrival of plasma flows in the region of strong magnetic fields. For plasma with heavier ions, this time increases, so that the reverse currents appeared later.

Nevertheless, the more rapid decrease in the current in the peripheral regions of the sheet compared to the central region of the current sheet was also, in all likelihood, caused by the appearance of currents in the opposite direction. However, far from the lateral ends of the sheet, both the plasma velocity and the normal component of the magnetic field are significantly smaller than at the lateral ends of the sheet. As a result, the reverse currents that arose here were smaller in magnitude than at the edges of the sheet and were not directly observed, but led to the effect of a faster decrease in the density of the main current than in the center. In turn, a decrease in the current density and, as a consequence, a decrease in the tangential component of the magnetic field at late moments of time caused a decrease in the forces that previously led to the compression of the current and plasma within the sheet. As a result, a 'thickening' of the current sheet occurred.

Thus, the generation of currents flowing in the opposite direction was manifested both explicitly and implicitly. In the former case, reverse currents were directly recorded, and, in the latter case, a faster decrease in the density of the main current and thickening of the peripheral areas of the sheet occurred.

Excitation of currents in the opposite direction should lead to a change in the structure of electrodynamic forces and, as a result, can exert a significant effect on the dynamics of plasma flows. As a result of the change in the direction of the current $I_z(x)$ at the lateral edges of the sheet, according to Eqn (20), Ampere forces arose, which were directed from the periphery to the middle of the sheet, i.e., towards the forces in the central region [116, 117]. Although the reverse currents are relatively small, the Ampere forces at the edges of the sheet turned out to be comparable in absolute value to or even greater than the forces in the central region of the sheet that accelerated the plasma in the direction from the middle of the sheet to its lateral edges (Fig. 20) [118].

The electrodynamic forces (braking forces) that arose at the edges of the sheet began to impede the further movement of the plasma flows and should have led to a noticeable slowing down of the movement of the plasma flows or even to

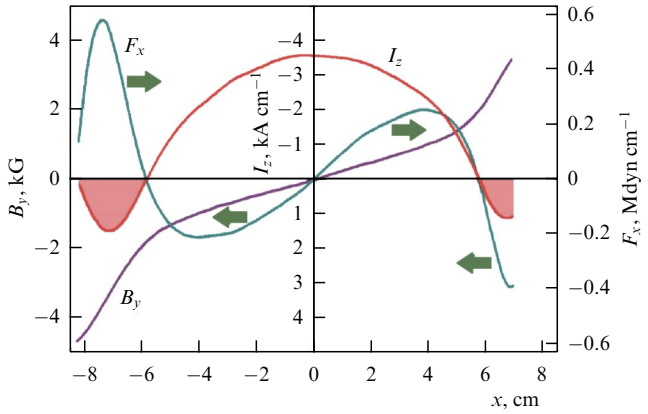

Figure 20. Distributions along current sheet width of linear current density $I_z(x)$, normal component of current sheet magnetic field $B_y(x)$, and Ampere forces $F_x(x)$. Arrows show directions of Ampere forces, $t = 4.5$ μs. Experimental conditions: see caption to Fig. 17a.

the cessation of the movement of these flows. Probably, this effect is associated with the nature of the change in the energy of the plasma flows W_x over time, when, after the growth stage and reaching a certain maximum value, the energy W_x decreased rather rapidly (Fig. 18b).

It should be emphasized that in all the studied modes the evolution of the plasma flow energy had a similar character [107, 108, 119, 120]. The growth of the energy of the directed plasma motion W_x began with a certain delay after the formation of the current sheet; W_x quickly increased and reached a maximum value, several times exceeding the thermal energy of the plasma. Then, the energy of the directed plasma motion rapidly decreased. The moments of time when the plasma acceleration began and the maximum energy was reached and the value of the maximum energy depended on the specific conditions under which the current sheet was formed.

The energy of the directed plasma motion was acquired due to the work of the Ampere forces along the acceleration length. In [117], the work of the Ampere forces operating in opposite directions along the surface of the current sheet, which should have caused both the acceleration and deceleration of the plasma flows, was analyzed in detail. As a result, a spatiotemporal correlation was revealed between the work of the Ampere forces, on the one hand, and the evolution of the energy of accelerated plasma flows W_x, on the other hand, for different current sheets formed in plasma with He, Ar, and Kr ions [116, 117].

Thus, the excitation of reverse currents in current sheets and the appearance of significant braking forces caused by these currents makes it possible to explain the nature of the change in the energy of plasma flows W_x over time, when, after the growth stage and reaching a certain maximum value, the energy decreased rather quickly.

This implies that the reverse currents that arose in the current sheet due to the movement of plasma flows then cause braking or even cessation of the movement of such flows. Note that this effect is a manifestation of the general rule of E.H. Lenz, according to which "the induction current always has such a direction that it weakens the effect of the cause that excites this current."

In general, the deceleration of plasma flows caused by the generation of currents in the opposite direction should manifest itself when fast plasma flows penetrate into regions with a strong transverse magnetic field. Apparently, similar phenomena can take place in Earth's magnetosphere when fast plasma flows enter a region of a strong (dipole) magnetic field. Satellite observations show that high-speed plasma flows that propagate from the tail region of the magnetosphere towards Earth consist of individual plasma jets with scales of several thousand km and a duration of 5–10 s (Bursty Bulk Flows; BBFs) (see, for example, [121–124]). A statistical analysis of the velocities of plasma flows shows that the flows decelerate as they approach Earth when penetrating into the region of a strong magnetic field of Earth's dipole [125].

Using multi-satellite missions that measured magnetic fields at spatially separated points in the magnetospheric current sheet, currents of the opposite direction were also detected, which should affect the dynamics of plasma flows (see, for example, [126, 127]). Based on such data, it can be assumed that one of the reasons for the slowing down and destruction of high-speed plasma flows propagating in the magnetosphere towards Earth may be the excitation of currents of the opposite direction. This indicates the unity of the basic physical processes occurring in the tail region of Earth's magnetosphere and in laboratory experiments, which was noted in some studies [102, 103, 128–131].

11. Conclusions

This review is dedicated to the centenary of the birth of Sergei Ivanovich Syrovatskii, an outstanding theoretical physicist, who obtained fundamental results in various fields of physics, including magnetohydrodynamics [132], cosmic ray astrophysics (which was the subject of many joint studies by S.I. Syrovatskii and V.L. Ginzburg, including reviews [133, 134] and monograph [135]) solar physics [136], and plasma physics.

The processes occurring on the Sun, and especially the physics of solar flares and other flare phenomena in plasma, attracted Sergei Ivanovich's attention in the 1960s. Already in the first studies devoted to the problems of solar activity and the acceleration of charged particles in nonstationary plasma [6, 7], S.I. Syrovatskii showed that plasma flows with a frozen-in magnetic field in the vicinity of the zero lines of the magnetic field should lead to a concentration of magnetic energy and electric current, which takes the form of a current sheet. The flash itself can occur during the rapid destruction (rupture) of the sheet, when the accumulated magnetic energy is converted into kinetic and thermal energy of the plasma, into streams of accelerated particles and radiation.

Sergei Ivanonich Syrovatskii and Vitaly Lazarevich Ginzburg.

Sergei Ivanonich Syrovatskii and Anna Glebovna Frank

Based on these concepts, experimental studies were started in the accelerator laboratory of the Lebedev Physical Institute, which were carried out in direct contact with and under the influence of theoretical ideas and concepts. The experimental results confirmed the predictions of the theory: at a sufficiently high plasma conductivity, a neutral current sheet was formed for the first time in laboratory conditions, and in subsequent series of experiments, a current sheet rupture was realized, accompanied by the generation of accelerated particles. Thus, S.I. Syrovatskii's concept of current sheets as the basis for flare phenomena in plasma was convincingly confirmed by experiment.

The content of this review shows that at present many of S.I. Syrovatskii's ideas are still relevant and are confirmed experimentally. One brilliant example is the possible appearance of currents of the opposite direction in current sheets, which was first predicted in S.I. Syrovatskii's theoretical work [10]. Then reverse currents were discovered in laboratory current sheets [110, 111, 115] and, comparatively recently, by satellite observations in Earth's magnetosphere [126, 127]. It turned out that reverse currents play an important role in the dynamics of plasma flows accelerated in current sheets [117].

It should also be noted that S.I. Syrovatskii's studies in the MHD theory of current sheets were to a large extent the starting point for the modern development of the theory of thin current sheets in collisionless plasma (see [137, 138] and the references cited there).

It should be emphasized that the study of current sheets in laboratory experiments is an important part of the general problem of converting magnetic energy into other types of energy. Recently, the spectrum of laboratory studies of the dynamics of current sheets and magnetic reconnection processes has significantly expanded (see [139] and the references cited there). Along with the study of basic physical problems, considerable attention is devoted to issues of laboratory modeling of phenomena occurring in outer space (see, for example, [128–131, 140, 141]).

The key element of the formation of current sheets with a significant content of magnetic energy is to create the condition for freezing the magnetic field into the plasma at the limited scale of laboratory installations. Most importantly, it should be done under the conditions of the development of plasma instabilities during the excitation of electric current, which causes the transition of the plasma to a turbulent regime with anomalously low conductivity. Our experiments conducted in 2D magnetic configurations with zero lines [18, 22] have shown that a satisfactory solution to this problem can be obtained with an appropriate choice of the initial conditions in which current sheets are formed.

These conditions should be determined first and foremost when studying the options for implementing flare processes in current sheets formed in 3D magnetic configurations, which is currently an urgent and high priority task of experimental research conducted in the Plasma Physics Department of the General Physics Institute of the Russian Academy of Sciences.

Gordon Conference Magnetic Reconnection in Space and Laboratory Plasmas (June 20–24, 1977, Wolfeboro, New Hampshire, USA). First row (sitting): 4th from left — S.I. Syrovatskii, 7th from left — A.G. Frank.

References

1. Giovanelli R G *Mon. Not. R. Astron. Soc.* **108** 163 (1948)
2. Dungey J W *Philos. Mag.* **44** 725 (1953)
3. Sweet P A *Nuovo Cimento Suppl.* **8** (Suppl. 2) 188 (1958)
4. Parker E N *Astrophys. J. Suppl.* **8** 177 (1963)
5. Petschek H E, in *The Physics of Solar Flares. Proc. of the AAS–NASA Symp. 28–30 October, 1963, Greenbelt, MD* (Ed. W N Hess) (Washington, DC: National Aeronautics and Space Administration, Science and Technical Information Division, 1964) p. 425
6. Syrovatskii S I *Sov. Astron.* **10** 270 (1966); *Astron. Zh.* **43** 340 (1966)
7. Syrovatskii S I *Sov. Phys. JETP* **23** 754 (1966); *Zh. Eksp. Teor. Fiz.* **50** 1133 (1966)
8. Imshennik V S, Syrovatskii S I *Sov. Phys. JETP* **25** 656 (1967); *Zh. Eksp. Teor. Fiz.* **52** 990 (1967)
9. Syrovatskii S I *Sov. Phys. JETP* **27** 763 (1968); *Zh. Eksp. Teor. Fiz.* **54** 1422 (1968)
10. Syrovatskii S I *Sov. Phys. JETP* **33** 933 (1971); *Zh. Eksp. Teor. Fiz.* **60** 1727 (1971)
11. Gerlach N I, Syrovatskii S I, in *Neutral Current Sheets in Plasmas* (Proc. (Trudy) of the P.N. Lebedev Phys. Inst., Vol. 74, Ed. N G Basov) (New York: Consultants Bureau, 1976) p. 73, https://doi.org/10.1007/978-1-4615-8564-0_3; Translated from Russian: in *Neitral'nye Tokovye Sloi v Plazme* (Tr. Fiz. Inst. Akad. Nauk SSSR, Vol. 74, Ed. N G Basov) (Moscow: Nauka, 1974) p. 73
12. Syrovatskii S I, in *Neutral Current Sheets in Plasmas* (Proc. (Trudy) of the P.N. Lebedev Phys. Inst., Vol. 74, Ed. N G Basov) (New York: Consultants Bureau, 1976) p. 1, https://doi.org/10.1007/978-1-4615-8564-0_1; Translated from Russian: in *Neitral'nye Tokovye Sloi v Plazme* (Tr. Fiz. Inst. Akad. Nauk SSSR, Vol. 74, Ed. N G Basov) (Moscow: Nauka, 1974) p. 3
13. Somov B V, Syrovatskii S I, in *Neutral Current Sheets in Plasmas* (Proc. (Trudy) of the P.N. Lebedev Phys. Inst., Vol. 74, Ed. N G Basov) (New York: Consultants Bureau, 1976) p. 13, https://doi.org/10.1007/978-1-4615-8564-0_2; Translated from Russian: in *Neitral'nye Tokovye Sloi v Plazme* (Tr. Fiz. Inst. Akad. Nauk SSSR, Vol. 74, Ed. N G Basov) (Moscow: Nauka, 1974) p. 14
14. Bratenahl A, Yeates C M *Phys. Fluids* **13** 2696 (1970)
15. Ohhyabu N, Kawashima N *J. Phys. Soc. Jpn.* **33** 496 (1972)
16. Syrovatskii S I, Frank A G, Khodzhaev A Z, in *Proc. of the 4th European Conf. on Controlled Fusion, Rome, 1970*, p. 66
17. Syrovatskii S I, Frank A G, Khodzhaev A Z *Sov. Phys. Tech. Phys.* **18** 580 (1973); *Zh. Tekh. Fiz.* **43** 912 (1973)
18. Frank A G, in *Neutral Current Sheets in Plasmas* (Proc. (Trudy) of the P.N. Lebedev Phys. Inst., Vol. 74, Ed. N G Basov) (New York: Consultants Bureau, 1976) p. 107, https://doi.org/10.1007/978-1-4615-8564-0_5; Translated from Russian: in *Neitral'nye Tokovye Sloi v Plazme* (Tr. Fiz. Inst. Akad. Nauk SSSR, Vol. 74, Ed. N G Basov) (Moscow: Nauka, 1974) p. 108
19. Demidov B A, Elagin N I, Fanchenko S D *Sov. Phys. Dokl.* **12** 467 (1967); *Dokl. Akad. Nauk SSSR* **174** 327 (1967)
20. Hamberger S M, Friedman M *Phys. Rev. Lett.* **21** 674 (1968)
21. Friedman M, Hamberger S M *Solar Phys.* **8** 104 (1969)
22. Syrovatskii S I, Frank A G, Khodzhaev A Z *JETP Lett.* **15** 94 (1972); *Pis'ma Zh. Eksp. Teor. Fiz.* **15** 138 (1972)
23. Stenzel R L, Gekelman W *J. Geophys. Res.* **86** 649 (1981)
24. Biskamp D *Phys. Fluids* **29** 1520 (1986)
25. Furth H P, Killen J, Rosenbluth M N *Phys. Fluids* **6** 459 (1963)
26. Laval G, Pellat R, Vuillemin M, in *Plasma Physics and Controlled Nuclear Fusion Research. Proc. of a Conf., September 6–10, 1965* Vol. 2 (Vienna: Intern. Atomic Energy Agency, 1966) p. 259
27. Kirii N P, Markov V S, Syrovatskii S I, Frank A G, Khodzhaev A Z, in *Vspyshechnye Protsessy v Plazme* (Flare Processes in Plasma) (Tr. Fiz. Inst. Akad. Nauk SSSR, Vol. 110, Ed. V L Ginzburg) (Moscow: Nauka, 1979) p. 121
28. Bogdanov S Yu et al. *Izv. Akad. Nauk SSSR Ser. Fiz.* **44** 2469 (1980)
29. Bogdanov S Yu et al. *Sov. J. Plasma Phys.* **1** 73 (1975); *Fiz. Plazmy* **1** 133 (1975)
30. Dreiden G V et al. *Sov. Tech. Phys. Lett.* **1** 68 (1975); *Pis'ma Zh. Tekh. Fiz.* **1** 141 (1975)
31. Dreiden G V et al. *Sov. J. Plasma Phys.* **3** 26 (1977); *Fiz. Plazmy* **3** 45 (1977)
32. Ostrovsky Yu I, Butusov M M, Ostrovskaya G V *Interferometry by Holography* (Springer Series in Optical Sciences, Vol. 20) (Berlin: Springer-Verlag, 1980) https://doi.org/10.1007/978-3-540-39008-4; Translated from Russian: *Golografic heskaya Intereferometriya* (Moscow: Nauka, 1977)
33. Syrovatskii S I *Bull. USSR Acad. Sci. Phys. Ser.* **43** (4) 17 (1980); *Izv. Akad. Nauk SSSR Ser. Fiz.* **43** 695 (1979)
34. Syrovatskii S I *Bull. USSR Acad. Sci. Phys. Ser.* **39** (2) 96 (1975); *Izv. Akad. Nauk SSSR Ser. Fiz.* **39** 359 (1975)
35. Syrovatskii S I, in *Vspyshechnye Protsessy v Plazme* (Flare Processes in Plasma) (Trudy Fiz. Inst. Akad. Nauk SSSR, Vol. 110, Ed. V L Ginzburg) (Moscow: Nauka, 1979) p. 5
36. Bulanov S V, Sasorov P V, Syrovatskii S I *JETP Lett.* **26** 565 (1977); *Pis'ma Zh. Eksp. Teor. Fiz.* **26** 729 (1977)
37. Bulanov S V, Sasorov P V *JETP Lett.* **27** 521 (1978); *Pis'ma Zh. Eksp. Teor. Fiz.* **27** 554 (1978)
38. Bulanov S V, Sakai J I, Syrovatskii S I *JETP Lett.* **28** 177 (1978); *Pis'ma Zh. Eksp. Teor. Fiz.* **28** 193 (1978)
39. Kirii N P et al. *Sov. J. Plasma Phys.* **3** 303 (1977); *Fiz. Plazmy* **3** 538 (1977)
40. Frank A G, in *Plasma Physics and Plasma Electronics* (Ed. L M Kovrizhnykh) (Commack, NY: Nova Science Publ., 1989) p. 131; Translated from Russian: in *Voprosy Fiziki Plazmy i Plazmennoi Elektroniki* (Problems of Plasma Physics and Plasma Electronics) (Tr. Fiz. Inst. Akad. Nauk SSSR, Vol. 160, Ed. L M Kovrizhnykh) (Moscow: Nauka, 1985) p. 93
41. Bogdanov S Yu et al. *J. Phys. Colloq.* **40** C7-221 (1979)
42. Bogdanov S Yu, Frank A G, Markov V S, in *Proc. of the XV Intern. Conf. on Phenomena in Ionized Gases, ICPIG-15, Minsk, 1981* Pt. 1 (Minsk, 1981) p. 0504
43. Bogdanov S Yu, Markov V S, Frank A G *JETP Lett.* **35** 290 (1982); *Pis'ma Zh. Eksp. Teor. Fiz.* **35** 232 (1982)
44. Bogdanov S Yu et al. *Phys. Scr.* **30** 282 (1984)
45. Dreiden G V et al. *Sov. J. Plasma Phys.* **4** 6 (1978); *Fiz. Plazmy* **4** 14 (1978)
46. Dreiden G V et al. *Sov. Phys. Tech. Phys.* **26** 1072 (1981); *Zh. Tekh. Fiz.* **51** 1850 (1981)
47. Bogdanov S Yu et al. *Sov. J. Plasma Phys.* **18** 659 (1992); *Fiz. Plazmy* **18** 1269 (1992)
48. Altyntsev A T et al. *Sov. J. Plasma Phys.* **4** 8 (1978); *Fiz. Plazmy* **4** 18 (1978)
49. Altyntsev A T, Krasov V I *Sov. Phys. Tech. Phys.* **22** 25 (1977); *Zh. Tekh. Fiz.* **47** (1) 44 (1977)
50. Bulanov S V, Sasorov P V *Sov. Astron.* **19** 464 (1976); *Astron. Zh.* **52** 763 (1975)
51. Bogdanov S Yu, Markov V S, Frank A G *JETP Lett.* **51** 638 (1990); *Pis'ma Zh. Eksp. Teor. Fiz.* **51** 563 (1990)
52. Švestka Z *Solar Flares* (Geophysics and Astrophysics Monographs, Vol. 8) (Dordrecht: D. Reidel, 1976) https://doi.org/10.1007/978-94-010-1459-5
53. Syrovatskii S I *Vestn. Akad. Nauk SSSR* (10) 33 (1977)
54. Frank A G et al., in *Proc. XVII Intern. Conf. on Phenomena in Ionized Gases, ICPIG-17, Budapest, 8–12 July 1985* Vol. 1 (Eds J S Bakos, Z Sörlei) (Budapest: Koezponti Fizikai Kutato Intezet, 1985) p. 102
55. Frank A G et al., in *Analytical Methods for Optical Tomography* (Proc. SPIE, Vol. 1843, Ed. G G Levin) (Bellingham, WA: SPIE, 1991) p. 19
56. Velikanova L G et al. *Sov. J. Plasma Phys.* **18** 803 (1992); *Fiz. Plazmy* **18** 1545 (1992)
57. Kirii N P, Markov V S, Frank A G *JETP Lett.* **48** 459 (1988); *Pis'ma Zh. Eksp. Teor. Fiz.* **48** 419 (1988)
58. Kirii N P, Markov V S, Frank A G *JETP Lett.* **56** 82 (1992); *Pis'ma Zh. Eksp. Teor. Fiz.* **56** 82 (1992)
59. Beigman I L et al. *J. Appl. Spectrosc.* **54** 761 (1991); *Zh. Prikl. Spektroskop.* **54** 1021 (1991)
60. Bogdanov S Yu, Kirii N P, Frank A G, in *Magnitnoe Peresoedinenie v Dvumernykh i Trekhmernykh Konfiguratsiyakh* (Magnetic Reconnection in 2D and 3D Configurations) (Tr. Inst. Obshchei Fiziki Ross. Akad. Nauk, Vol. 51, Ed. L M Kovrizhnykh) (Moscow: Nauka. 1996) p. 3
61. Frank A G et al. *Contrib. Plasma Phys.* **36** 667 (1996)
62. Bogdanov S Yu et al. *Sov. J. Plasma Phys.* **18** 667 (1992); *Fiz. Plazmy* **18** 1283 (1992)

63. Syrovatskii S I *Sov. Astron. Lett.* **2** 13 (1976); *Pis'ma Astron. Zh.* **2** 35 (1976)
64. Syrovatskii S I *Priroda* (2) 143 (1978)
65. Sedov L I *Similarity and Dimensional Methods in Mechanics* (Moscow: Mir Publ., 1982); Translated from Russian: *Metody Podobiya i Razmernosti v Mekhanike* (Moscow: Nauka, 1967)
66. Alfvén H, Fälthammar C-G *Cosmical Electrodynamics* (Oxford: Oxford Univ. Press, 1963); Translated into Russian: *Kosmicheskaya Elektrodinamika* (Moscow: Mir Publ., 1967)
67. Schindler K, in *The Magnetosphere*: *Magnetospheric Physics. Proc. of a Symp., Washington, DC, 3–13 September 1968* (Eds D J Williams, G D Mead) (Washington, DC: American Geophysical Union, 1969); Translated into Russian: *Fizika Magnitosfery* (Eds D J Williams, G D Mead) (Moscow: Mir, 1972) p. 69
68. Baranov V B *Cosmic Res.* **7** 98 (1969); *Kosm. Issled.* **7** 109 (1969)
69. Podgornyi I M, Sagdeev R Z *Sov. Phys. Usp.* **12** 445 (1970); *Usp. Fiz. Nauk* **98** 409 (1969)
70. Bulanov S V, Dogiel V A, Frank A G *Phys. Scr.* **29** 66 (1984)
71. Bulanov S V, Dogel V A, Frank A G *Sov. Astron. Lett.* **10** 59 (1984); *Pis'ma Astron. Zh.* **10** 149 (1984)
72. Sturrock P A (Ed.) *Solar Flares*: *A Monograph from Skylab Solar Workshop II, Boulder, 1976–1977* (Boulder, CO: Colorado Associated Univ. Press, 1980)
73. Syrovatskii S I *Vestn. Akad. Nauk SSSR* (3) 31 (1973)
74. Syrovatskii S I *Izv. Akad. Nauk SSSR Ser. Fiz.* **41** 1782 (1977)
75. Kadomtsev B B *Usp. Fiz. Nauk* **151** 3 (1987); *Rep. Prog. Phys.* **50** 115 (1987)
76. Syrovatskii S I *Annu. Rev. Astron. Astrophys.* **19** 163 (1981)
77. Rosenau P *Phys. Fluids* **22** 849 (1979)
78. Bulanov S V, Olshanetskii M A *Sov. J. Plasma Phys.* **11** 425 (1985); *Fiz. Plazmy* **11** 727 (1985)
79. Lau Y-T, Finn J M *Astrophys. J.* **350** 672 (1990)
80. Green J M *Phys. Fluids B* **5** 2355 (1993)
81. Bulanov S V, Frank A G *Sov. J. Plasma Phys.* **18** 795 (1992); *Fiz. Plazmy* **18** 1535 (1992)
82. Bogdanov S Yu et al. *JETP Lett.* **59** 537 (1994); *Pis'ma Zh. Eksp. Teor. Fiz.* **59** 510 (1994)
83. Frank A G, Bogdanov S Yu, Burilina V B *Bull. Russ. Acad. Sci. Phys.* **59** 1331 (1995); *Izv. Ross. Akad. Nauk Ser. Fiz.* **59** (8) 41 (1995)
84. Bogdanov S Yu, Frank A G, Kyrie N P, in *Advances in Solar Physics*: *Proc. of the Seventh European Meeting on Solar Physics, Catania, Italy, 11–15 May 1993* (Lecture Notes in Physics, Vol. 432, Eds G Belvedere, M Rodonò, G M Simnett) (Berlin: Springer-Verlag, 1994) p. 231
85. Frank A G *Plasma Phys. Control. Fusion* **41** A687 (1999)
86. Frank A G, Bogdanov S Yu *Earth Planets Space* **53** 531 (2001)
87. Bogdanov S Yu et al. *JETP Lett.* **71** 53 (2000); *Pis'ma Zh. Eksp. Teor. Fiz.* **71** 78 (2000)
88. Bogdanov S Yu et al. *Plasma Phys. Rep.* **28** 549 (2002); *Fiz. Plazmy* **28** 594 (2002)
89. Frank A G et al., in *Plasmas in the Laboratory and in the Universe*: *New Insights and New Challenges* (AIP Conf. Proc., Vol. 703, Eds G Bertin, D Farina, R Pozzoli) (Melville, NY: AIP, 2004) p. 431
90. Frank A G et al. *Phys. Plasmas* **12** 052316 (2005)
91. Frank A G *Phys. Usp.* **53** 941 (2010); *Usp. Fiz. Nauk* **180** 982 (2010)
92. Frank A G *Plasma Phys. Rep.* **48** 574 (2022)
93. Bogdanov S Yu et al. *Plasma Phys. Rep.* **33** 435 (2007); *Fiz. Plazmy* **33** 483 (2007)
94. Bogdanov S Yu et al. *Plasma Phys. Rep.* **32** 1034 (2006); *Fiz. Plazmy* **32** 1121 (2006)
95. Frank A, Bugrov S, Markov V *Phys. Lett. A* **373** 1460 (2009)
96. Frank A G, Satunin S N *Plasma Phys. Rep.* **44** 190 (2018); *Fiz. Plazmy* **44** 144 (2018)
97. Frank A G et al. *Phys. Lett. A* **348** 318 (2006)
98. Bogdanov S Yu et al. *Plasma Phys. Rep.* **33** 930 (2007); *Fiz. Plazmy* **33** 1014 (2007)
99. Ostrovskaya G V, Frank A G *Plasma Phys. Rep.* **40** 21 (2014); *Fiz. Plazmy* **40** 24 (2014)
100. Frank A G, Satunin S N *JETP Lett.* **100** 75 (2014); *Pis'ma Zh. Eksp. Teor. Fiz.* **100** 83 (2014)
101. Frank A G, Bugrov S G, Markov V S *Phys. Plasmas* **15** 092102 (2008)
102. Frank A G et al. *Cosmic Res.* **55** 46 (2017); *Kosm. Issled.* **55** 48 (2017)
103. Yushkov E V et al. *Plasma Phys. Rep.* **44** 1126 (2018); *Fiz. Plazmy* **44** 983 (2018)
104. Frank A G, Satunin S N *Bull. Lebedev Phys. Inst.* **47** (2) 54 (2020); *Kratk. Soobshch. Fiz. FIAN* **47** (2) 28 (2020)
105. Frank A G et al., in *Opticheskie Svoistva Nizkotemperaturnoi Plazmy* (Optical Properties of Low-Temperature Plasma) (Encyclopedia of Low-Temperature Plasma, Ser.s B, Vol. 3-2, Pt. 1, Ed. V N Ochkin) (Moscow: Yanus-K, 2008) p. 335
106. Kyrie N P, Markov V S, Frank A G *Plasma Phys. Rep.* **36** 357 (2010); *Fiz. Plazmy* **36** 387 (2010)
107. Kyrie N P, Markov V S, Frank A G *JETP Lett.* **95** 14 (2012); *Pis'ma Zh. Eksp. Teor. Fiz.* **95** 17 (2012)
108. Kyrie N P, Frank A G *Plasma Phys. Rep.* **38** 960 (2012); *Fiz. Plazmy* **38** 1042 (2012)
109. Bogdanov S Yu, Frank A G, Markov V S, in *Proc. XVII Intern. Conf. on Phenomena in Ionized Gases, ICPIG-17, Budapest, 8–12 July 1985* Vol. 1 (Eds J S Bakos, Z Sörlei) (Budapest: Koezponti Fizikai Kutato Intezet, 1985) p. 67
110. Frank A G, Satunin S N *Plasma Phys. Rep.* **37** 829 (2011); *Fiz. Plazmy* **37** 889 (2011)
111. Frank A G, Kyrie N P, Satunin S N *Phys. Plasmas* **18** 111209 (2011)
112. Frank A G, in *Proc. European Conf. on Plasma Astrophysics* (EAS Publ. Ser., Vol. 58, Eds C Stehlé, C Joblin, L d'Hendecourt) (Geneva: European Astronomical Society, 2012) p. 57
113. Frank A G, Kyrie N P *Plasma Phys. Rep.* **43** 696 (2017); Translated from Russian: *Usp. Prikl. Fiz.* **3** 454 (2015)
114. Frank A G et al. *Plasma Phys. Rep.* **44** 551 (2018); *Fiz. Plazmy* **44** 483 (2018)
115. Frank A G, Satunin S N *JETP Lett.* **112** 623 (2020); *Zh. Eksp. Teor. Fiz.* **112** 667(2020)
116. Frank A et al. *Universe* **7** (11) 400 (2021)
117. Frank A G, Satunin S N *Plasma Phys. Rep.* **48** 10 (2022); *Fiz. Plazmy* **48** 12 (2022)
118. Frank A G, Savinov S A *Symmetry* **16** (1) 103 (2024)
119. Kyrie N P, Frank A G, Vasilkov D G *Plasma Phys. Rep.* **45** 325 (2019); *Fiz. Plazmy* **45** 313 (2019)
120. Kyrie N P, Savinov S A *Plasma Phys. Rep.* **47** 611 (2021)
121. Baumjohann W, Paschmann G, Luehr H *J. Geophys. Res.* **95** 3801 (1990)
122. Angelopoulos V et al. *J. Geophys. Res.* **97** 4027 (1992)
123. Shiokawa K, Baumjohann W, Haerendel G *Geophys. Res. Lett.* **24** 1179 (1997)
124. Birn J et al. *J. Geophys. Res.* **104** 19895 (1999)
125. Liu J et al. *J. Geophys. Res.* **119** 909 (2014)
126. Lu S et al. *J. Geophys. Res.* **121** 4269 (2016)
127. Frank A G et al. *Plasma Phys. Control. Fusion* **65** 095006 (2023)
128. Artemyev A V et al. *J. Geophys. Res.* **118** 2789 (2013)
129. Zelenyi L M et al. *Plasma Phys. Control. Fusion* **58** 054002 (2016)
130. Frank A G, Artemyev A V, Zelenyi L M *J. Exp. Theor. Phys.* **123** 699 (2016); *Zh. Eksp. Teor. Fiz.* **150** 807 (2016)
131. Frank A G et al. *Astron. Rep.* **68** 406 (2024); *Astron. Zh.* **101** 366 (2024)
132. Syrovatskii S I *Usp. Fiz. Nauk* **62** 247 (1957)
133. Ginzburg V L, Syrovatskii S I *Sov. Phys. Usp.* **3** 504 (1961); *Usp. Fiz. Nauk* **71** 411 (I960)
134. Ginzburg V L, Syrovatskii S I *Sov. Phys. Usp.* **9** 223 (1966); *Usp. Fiz. Nauk* **88** 485 (1966)
135. Ginzburg V L, Syrovatskii S I *The Origin of Cosmic Rays* (Oxford: Pergamon Press, 1964); Translated from Russian: *Proiskhozhdenie Kosmicheskikh Luchei* (Moscow: Izd. AN SSSR, 1963)
136. Somov B V, Syrovatskii S I *Sov. Phys. Usp.* **19** 813 (1976); *Usp. Fiz. Nauk* **120** 217 (1976)
137. Zelenyi L M et al. *Phys. Usp.* **59** 1057 (2016); *Usp. Fiz. Nauk* **186** 1153 (2016)
138. Zelenyi L M et al. *Phys. Usp.* **68** (8) (2025) https://doi.org/10.3367/UFNe.2025.03.039950; *Usp. Fiz. Nauk* **195** 807 (2025)
139. Yamada M, Kurlsrud R, Ji H *Rev. Mod. Phys.* **82** 603 (2010)
140. Koepke M E *Rev. Geophys.* **46** RG3001 (2008)
141. Zweibel E G, Yamada M *Annu. Rev. Astron. Astrophys.* **47** 291 (2009)